

0.51
97te

1194

SCHOOL OF CIVIL ENGINEERING

INDIANA

DEPARTMENT OF HIGHWAYS

JOINT HIGHWAY RESEARCH PROJECT

FHWA/IN/JHRP-87/2 -1

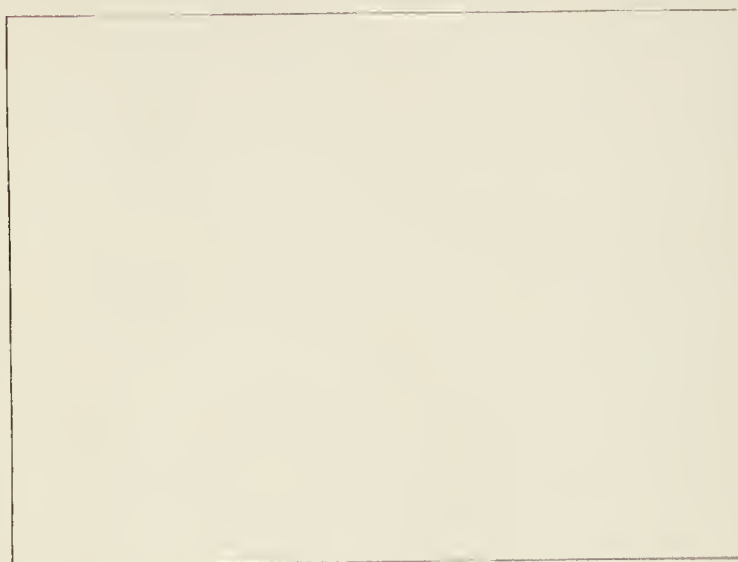
Final Report

BEHAVIOR OF MUCKS AND AMORPHOUS
PEATS AS EMBANKMENT FOUNDATIONS

Timothy Crowl and C. W. Lovell



PURDUE UNIVERSITY



JOINT HIGHWAY RESEARCH PROJECT

FHWA/IN/JHRP-87/2 -1

Final Report

BEHAVIOR OF MUCKS AND AMORPHOUS
PEATS AS EMBANKMENT FOUNDATIONS

Timothy Crowl and C. W. Lovell

FINAL REPORT

BEHAVIOR OF MUCKS AND AMORPHOUS PEATS AS EMBANKMENT FOUNDATIONS

To: H. L. Michael, Director
Joint Highway Research Project
May 26, 1987
Project: C-36-5P

From: C. W. Lovell, Research Engineer
Joint Highway Research Project
File: 6-6-16

Attached is a Final Report on the study, "Behavior of Mucks and Amorphous Peats as Embankment Foundations". The report is written by Timothy Crowl and C. W. Lovell.

These materials of very low shear strength and very high compressibility are seldom used as embankment foundations. However, the research proposes a technique for successful use for low embankments (+10 ft), where loading is in stages.

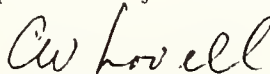
Stage height is controlled by suitable safety against bearing failure, lateral squeezing, embankment spreading, and rotational sliding. Strengths are determined at any stage of the construction by field vane shear measurements. Stage duration is determined by field pore pressure measurements.

Settlement prediction is produced by: laboratory creep tests, the Gibson-Lo model, and previous correlations between laboratory and field settlement measurements. Surcharge loading is usually required before a pavement may be placed on the embankment.

Examples of the proposed method are included, both with and without the inclusion of geotextiles.


The report is submitted for review, comment and acceptance in fulfillment of the referenced study.

Respectfully submitted,



C. W. Lovell
Research Engineer

cc: A.G. Altschaeffl	R.A. Howden	B.K. Partridge
J.M. Bell	M.K. Hunter	G.T. Satterly
M.E. Cantrall	J.P. Isenbarger	C.F. Scholer
W.F. Chen	J.F. McLaughlin	K.C. Sinha
W.L. Dolch	K.M. Mellinger	C.A. Venable
R.L. Eskew	R.D. Miles	T.D. White
J.D. Fricker	P.L. Owens	L.E. Wood
D.E. Hancher		



Digitized by the Internet Archive
in 2011 with funding from
LYRASIS members and Sloan Foundation; Indiana Department of Transportation

FINAL REPORT

BEHAVIOR OF MUCKS AND AMORPHOUS
PEATS AS EMBANKMENT FOUNDATIONS

by

Timothy Crowl
Graduate Instructor in Research

and

C. W. Lovell
Research Engineer

Joint Highway Research Project

Project No.: C-36-5P
File No.: 6-6-16

Prepared for an Investigation
Conducted by the

Joint Highway Research Project
Engineering Experiment Station
Purdue University

in cooperation with the

Indiana Department of Highways

and the

U.S. Department of Transportation
Federal Highway Administration

The opinions, findings and conclusions expressed in this publication are those of the authors and not necessarily those of the Federal Highway Administration.

Purdue University
West Lafayette, Indiana
May 26, 1987

1. Report No. FHWA/IN/JHRP-87/2		2. Government Accession No.		3. Recipient's Catalog No.	
4. Title and Subtitle BEHAVIOR OF MUCKS AND AMORPHOUS PEATS AS EMBANKMENT FOUNDATIONS				5. Report Date May 26, 1987	
				6. Performing Organization Code	
7. Author(s) Timothy Crowl and C. W. Lovell				8. Performing Organization Report No. JHRP-87/2	
9. Performing Organization Name and Address Joint Highway Research Project Civil Engineering Building Purdue University West Lafayette, Indiana 47907				10. Work Unit No.	
				11. Contract or Grant No.	
12. Sponsoring Agency Name and Address Indiana Department of Highways State Office Building 100 North Senate Avenue Indianapolis, Indiana 46204				13. Type of Report and Period Covered Final Report	
				14. Sponsoring Agency Code	
15. Supplementary Notes Prepared in cooperation with the U.S. Department of Transportation, Federal Highway Administration					
16. Abstract The construction of highway embankments over deposits of amorphous peat and muck is made difficult by the low shear strengths, high compressibilities, and excessive amounts of creep typically associated with soils of this nature. This report begins with a review of the compression behavior of these soils, including a method for predicting embankment settlements from the results of laboratory tests. A soil testing program is then developed for the determination of parameters required for embankment design and construction. Field vane shear tests are recommended for the measurement of the undrained shear strength, and creep tests are recommended for calculation of the parameters required for settlement prediction. The report concludes with the presentation of a procedure for design and construction of embankments over amorphous peats and mucks. The procedure relies upon the use of stage loading, preloading, and in some instances geotextiles, to overcome the problems ordinarily encountered during construction over such soft soils. Design examples illustrating this procedure are provided.					
17. Key Words peat, muck, embankment, foundation, creep, settlement, stage construction, surcharge, geotextiles			18. Distribution Statement No restrictions. This document is available to the public through the National Technical Information Service, Springfield, VA 22161		
19. Security Classif. (of this report) Unclassified		20. Security Classif. (of this page) Unclassified		21. No. of Pages 126	
				22. Price	

ACKNOWLEDGEMENTS

Special thanks are extended to Mr. David Frost for the advice and support provided during this project. The authors wish to express their gratitude to Mr. Barry Christopher for his assistance and recommendations. Thanks are also due to Mrs. Cathy Ralston and Mrs. Kathie Roth for their help in preparing this report, and for their support and encouragement.

Financial support for this research was provided by the Indiana Department of Highways and the Federal Highway Administration. The research was administered through the Joint Highway Research Project, Indianapolis, Indiana.

TABLE OF CONTENTS

	Page
LIST OF TABLES.....	vi
LIST OF FIGURES.....	vii
LIST OF SYMBOLS AND ABBREVIATIONS.....	ix
HIGHLIGHT SUMMARY.....	xi
CHAPTER I-INTRODUCTION.....	1
Introduction.....	1
Scope.....	3
CHAPTER II-LITERATURE REVIEW.....	4
Compression of Organic Materials.....	4
Settlement Prediction.....	6
Field Inconsistencies.....	6
Prediction Model Inconsistencies.....	8
Gibson-Lo Model.....	10
Yield Envelope Concept.....	18
Construction Techniques.....	23
Stage Loading.....	23
Berms.....	23
Sand Drains.....	24
Geotextiles.....	25
CHAPTER III-TESTING PROGRAM.....	32
Introduction.....	32
Materials Studied.....	32
Production of Samples for Laboratory Testing.....	33
Creep Testing.....	38
K Triaxial Testing.....	45
Field Vane Shear Tests.....	53
CHAPTER IV-PROCEDURE FOR DESIGN AND CONSTRUCTION.....	62
Site Exploration.....	62
Embankment Design.....	64
Embankments without Geotextile Reinforcement.....	65

Overall Bearing Capacity.....	66
Lateral Squeeze.....	66
Embankment Spreading.....	67
Rotational Failure.....	70
Geotextile Reinforced Embankments.....	71
Overall Bearing Capacity.....	71
Lateral Squeeze.....	71
Rotational Failure.....	72
Embankment Spreading.....	72
Limit Fabric Deformation.....	73
Stage Loading.....	75
Preloading.....	77
Field Observations.....	81
Embankment Materials.....	82
Construction Sequence.....	82
CHAPTER V-CONCLUSIONS AND RECOMMENDATIONS.....	86
Conclusions.....	86
Recommendations.....	87
LIST OF REFERENCES.....	89
APPENDICES	
Appendix A: Creep Test Results.....	93
Appendix B: K ₀ Triaxial Test Check List.....	102
Appendix C: Computer Programs.....	106
Appendix D: Design Examples.....	110
Appendix E: Negative Numbers for Contact Prints.....	131

LIST OF TABLES

Table	Page
3.1 Soil Characteristics.....	34
3.2 Values of $C_{\alpha_{\epsilon}}$	44
3.3 K_o Triaxial Test Results.....	54
3.4 Values of Undrained Shear Strength from Field Vane Shear Tests.....	57

LIST OF FIGURES

Figure	Page
2.1 Primary Compressibility versus Stress Level. From Edil and Mochtar (1984).....	13
2.2 Secondary Compressibility versus Stress Level. From Edil and Mochtar (1984).....	14
2.3 Correction Curve for Laboratory Values of Secondary Compressibility. From Edil and Mochtar (1984).....	15
2.4 Dependency of Rate Factor for Secondary Compression on Average Strain Rate. From Edil and Mochtar (1984).....	16
2.5 Major Features of Yield Envelope. From Watson et al. (1984).....	19
2.6 Effective Stress Path during Multi-Stage Loading. From Watson et al. (1984).....	22
3.1 Slurry Consolidometer.....	37
3.2 Slurry Consolidometer Adapted for Production of Creep Test Samples.....	39
3.3 Strain versus Logarithm Time, Creep Test OL-6-2....	41
3.4 Strain versus Logarithm Time, Creep Test LR-6-1....	42
3.5 Calculation of $C_{\alpha_{\epsilon}}$	43
3.6 New K_0 Triaxial Cap, Top View.....	49
3.7 New K_0 Triaxial Cap, Bottom View.....	50
3.8 K_0 Triaxial Apparatus.....	51
3.9 Loading Time-Rate Correction Factor versus Plasticity Index for Undrained Shear Strength as Measured by the Field Vane. From Bjerrum et al. (1972).....	59

Figure	Page
4.1 Description of Variables in Equation 4.3.....	68
4.2 Embankment Spreading.....	69
4.3 Pore Pressure Transducer Installation From Slope Indicator Company.....	76
4.4 Plot of Log Strain Rate with Time from Laboratory Tests. From Lo, Bozozuk, and Law (1976).....	79
4.5 Inclinomater Type SGI. From Winterkorn and Fang (1975).....	83
4.6 Construction Sequence. From Barsvary et al. (1982).....	84
Appendix	
Figure	
A1 Strain versus Logarithm Time, Creep Test OL-3-1.....	94
A2 Strain versus Logarithm Time, Creep Test OL-6-1.....	95
A3 Strain versus Logarithm Time, Creep Test OL-9-1.....	96
A4 Strain versus Logarithm Time, Creep Test OL-9-2.....	97
A5 Strain versus Logarithm Time, Creep Test LR-3-1.....	98
A6 Strain versus Logarithm Time, Creep Test LR-6-2.....	99
A7 Strain versus Logarithm Time, Creep test LR-9-1.....	100
A8 Strain versus Logarithm Time, Creep Test LR-9-2.....	101
D1 Embankment Configuration for Design Example.....	111
D2 Revised Embankment Configuration for Design Example.....	113
D3 Plot of STABL Output for 10 Foot Embankment.....	116
D4 Plot of Logarithm Rate Versus Time, Creep Test OL-9-2.....	117
D5 Settlement Prediction for 10 Foot Embankment.....	120
D6 Plot of STABL Output for Surcharged Embankment.....	123
D7 Settlement Prediction for Surcharged Embankment.....	125

LIST OF SYMBOLS AND ABBREVIATIONS

ASTM	- American Society of Testing Materials
a	- primary compressibility, also one half of deposit thickness
B	- length of embankment (=1 ft for unit length)
b	- secondary compressibility
b_{field}	- field value of secondary compressibility
b_{lab}	- laboratory value of secondary compressibility
$C_{\alpha \epsilon}$	- modified coefficient of secondary compressibility
c	- undrained shear strength, see also s_u
c'	- effective cohesion
E_f	- minimum geotextile tensile modulus
E_{fr}	- minimum geotextile modulus to control rotational failure
K_o	- coefficient of lateral earth pressure at rest
K_s	- modulus of subgrade reaction
L	- one half of embankment base width
l	- lateral distance from crest to toe of embankment
N_c	- bearing capacity factor
P_a	- lateral earth pressure in cohesionless embankment
P_r	- force resisting embankment spreading
q	- ultimate bearing capacity
q_{all}	- allowable pressure

q_{app}	- applied pressure
s_u	- undrained shear strength, see also c
T_f	- required fabric strength
T_{fr}	- required tensile strength of fabric
t	- time
t_f	- time of last strain reading
$\Delta\sigma$	- applied stress increment
ϵ	- strain
ϵ_f	- last strain reading
ϵ_{max}	- maximum strain in geotextile along embankment centerline
γ	- unit weight of embankment soil
λ	- rheological parameter in Gibson-Lo model
$\frac{\lambda}{b}$	- rate factor for secondary compressibility
$(\frac{\lambda}{b})_{lab}$	- laboratory value of rate factor for secondary compressibility
$(\frac{\lambda}{b})_{field}$	- field value of rate factor for secondary compressibility.
ϕ'	- effective angle of internal friction
ϕ_{sf}	- soil fabric friction angle

HIGHLIGHT SUMMARY

The construction of highway embankments over deposits of amorphous peat and muck is made difficult by the low shear strengths, high compressibilities, and excessive amounts of creep typically associated with soils of this nature. This report begins with a review of the compression behavior of these soils, including a method for predicting embankment settlements from the results of laboratory tests. A soil testing program is then developed for the determination of parameters required for embankment design and construction. Field vane shear tests are recommended for the measurement of the undrained shear strength, and creep tests are recommended for calculation of the parameters required for settlement prediction. The report concludes with the presentation of a procedure for design and construction of low embankments (± 10 ft) over amorphous peats and mucks. The procedure relies upon the use of stage loading, preloading, and in some instances geotextiles, to overcome the problems ordinarily encountered during construction over such soft soils. Design examples illustrating this procedure are provided.

CHAPTER I-INTRODUCTION

INTRODUCTION

A large number of deposits of amorphous peat and muck are located within the State of Indiana. Many difficulties are encountered when highway embankments are constructed over these soft soils. In the past, highway engineers have relocated roadways to avoid construction over peat or muck. In other instances, the organic material was excavated and replaced with a more suitable material. However, neither of these methods are economical by modern standards, forcing highway departments to develop more sophisticated methods which allow construction directly across deposits of such materials.

Two characteristics associated with amorphous peats and mucks make them undesirable as materials for embankment foundations. Materials of this nature compress excessively when they are subjected to an applied load. A large portion of the compression is a result of the relatively high amounts of secondary compression associated with organic soils. These deformations occur over a long period of time, which compounds the problem. Deposits of these materials possess low preconsolidation pressures, so a large

compression response is likely even at low stress levels. Amorphous peats and mucks are also characterized by very low shear strengths. Shear failures, which are both expensive and time consuming to renovate, can occur very easily either during or after construction. Deposits of amorphous peat and muck are highly variable, so that representative values of compressibility and shear strength are difficult to define.

As a result of these typical characteristics, efforts to construct highway embankments over these materials have often resulted in poor performance in the form of excessive total settlements, large differential settlements, and shear failures. In addition, attempts to predict embankment settlements from the results of laboratory tests are often unsuccessful.

It is the aim of this project to develop a procedure for the design and construction of low embankments (± 10 ft) over amorphous peat and muck. This procedure will include the use of a soil testing program to determine parameters required during embankment construction. In addition, using the method for settlement prediction presented in this report, it is hoped that more reliable settlement predictions may be achieved.

SCOPE

This report will begin with a review of existing literature concerning the topic. Included will be a discussion of selected highlights of previous work performed at Purdue University by Gruen (1983) and Joseph (1986). Emphasis will be placed on settlement prediction and construction techniques.

Chapter 3 will describe the testing program developed for use during the design and construction of embankments over amorphous peat and muck. Sample preparation, testing procedures, and test results will be covered in this chapter. During this project, a major modification was required for the K_0 triaxial apparatus, and a discussion of this design is included.

The recommended design and construction procedure will be presented in Chapter 4. Material in this chapter will include a discussion of site exploration, implementation of the testing program, and subsequent embankment construction. In many instances on soft soils, geotextiles are used during embankment construction, and a discussion of the design of reinforced embankments is presented. Design examples will be included for unreinforced and geotextile reinforced embankments. This report will conclude with Chapter 5, which provides a summary of the content and recommendations for further research.

CHAPTER II-LITERATURE REVIEW

COMPRESSION OF ORGANIC MATERIALS

To date, there has been a large amount of effort expended to develop a better understanding of the compressibility characteristics of organic soils. Research has been performed in both the laboratory and the field to predict the behavior of these materials under an applied load. The primary goal of this research has been to increase the reliability of settlement estimates.

Organic materials display four modes of deformation when they are loaded (Gruen, 1983):

Instantaneous Strain: This mode occurs when the soil is initially loaded as a result of the elastic deformation of the soil mass. During this mode, gas that is trapped within the soil is also compressed or dissipated. Instantaneous strain occurs very quickly.

Primary Strain: Excess pore water pressures develop when a load is applied to the soil mass. During primary strain, deformation is a result of the dissipation of these pressures as the water is expelled from the pores. This strain mode occurs relatively quickly in

most instances, but accounts for a large amount of settlement.

Secondary Strain: This strain mode begins during primary strain and continues after excess pore water pressures have dissipated. The effective stresses between particles remain constant, implying that deformation is the result of creep. This strain mode continues for long periods of time, and is responsible for large amounts of settlement.

Tertiary Strain: This mode has been observed only in laboratory consolidation tests. Edil & Simon-Gilles (1986) state that there is no known evidence of tertiary compression occurring in the field. Tertiary strain is indicated by an increase in the rate of creep greater than the rate of secondary strain. Tertiary strain must ultimately return to secondary strain.

Dhowian & Edil (1980) state that at high consolidation pressures, the coefficients of secondary and tertiary compression approach the same value. This implies that secondary compression and tertiary compression occur simultaneously at high pressures. Dhowian & Edil offer no explanation for this mode of strain.

SETTLEMENT PREDICTION

There have been many attempts to predict the rates of settlement of embankments constructed over organic soils, with limited success. Inconsistencies between conditions in the laboratory and the field make accurate settlement prediction difficult. In addition, the models developed to make these predictions are approximate.

Field Inconsistencies

A number of discrepancies exist between laboratory and field conditions when these materials are loaded. Lefebvre et al. (1984) compared the results of laboratory tests and field performance for an embankment constructed on a fibrous peat. Two distinct trends were noted during this comparison. One trend indicated that the coefficient of secondary compression in the field was at least twice that exhibited under laboratory loading conditions. Also, the time for primary consolidation to occur in the field was less than that predicted using a one-dimensional theory of consolidation with the results from laboratory tests.

Lefebvre et al. (1984) attributed the larger field values of secondary compression to a number of factors. During oedometer tests, only vertical deformations are allowed, while field deformations are not purely one-dimensional. Any lateral movements will increase the amount

of vertical deformation, and may be mistaken as secondary compression. They also suggest that variations of the water table within the peat and the embankment materials increased compression. Any decrease in the elevation of the water table was accompanied by a decrease in pore water pressure. As a result, the effective stresses in the deposit were increased, inducing additional settlement. Snow loads during winter months were also responsible for increased settlements. Lefebvre et al. contend that a portion of the vertical deformation assumed to be secondary compression was actually primary compression caused by increased effective stresses.

The faster-than-predicted primary consolidation observed in the field was in part due to the use of the Terzaghi theory in making the prediction. Terzaghi theory does not take into account any secondary compression that occurs during primary consolidation. The observed discrepancy was also due to radial consolidation which occurred in the field, but was not allowed in consolidation tests conducted in the laboratory. In fact, for fibrous peat, horizontal permeability actually became larger than vertical permeability as the peat compressed. Lefebvre et al. (1984) also attribute the difference between field and laboratory consolidation times to the variation of the water table and the resulting change in effective stresses.

Other sources of error are a result of poorer compaction around measurement instruments placed in the fill, possibly affecting the observed settlements and pore pressures. In addition, the variability of the initial void ratio creates a range of initial compressibilities under low stresses. However, for loading greater than 20 kPa, the compressibilities were observed to converge to nearly the same value when an additional load was applied.

In most instances, deposits of amorphous peat and muck are underlain by thick deposits of soft clay or marl. Weber (1969) observed the field performance of an embankment constructed over a peat deposit. A layer of soft silty clay beneath the peat was observed to display long term compression. Weber felt that this compression was significant enough to cause the poor correlation between settlement predictions and field measurements.

Prediction Model Inconsistencies

In a report by Gruen (1983), a review was made of existing settlement prediction models for peats. None of the models considered account for settlement resulting from shear deformations. They state that shear deformations can comprise a large portion of settlement, so these predictive models provide approximate solutions at best.

Of all the models treated by Gruen, the Gibson-Lo model was chosen as the most useful. This model was the easiest to use, yet it was found to be as accurate as other models reviewed. In order to determine the accuracy of predictions from this model, consolidation tests were performed in the laboratory. Using the results of these tests, settlement predictions were made using the Gibson-Lo model for consolidation tests performed at other stress levels. Gruen found that predictions were reasonably accurate for stress levels less than or equal to approximately two times the stress level for tests used to make the predictions.

The Gibson-Lo model is a rheological model consisting of a Hookean spring in series with a Kelvin or Voigt element. The input parameters of this equation are strain-rate dependent. However, as Edil & Simon-Gilles (1986) discussed, the field strain rate during secondary compression is often two to three orders of magnitude lower than the laboratory strain rate, due to the large difference in thickness between laboratory samples and field deposits. Therefore, the Gibson-Lo model can not be used directly to predict field performance from the results of laboratory tests. A correlation between parameters obtained from laboratory and field loading must be used to make accurate predictions of field performance.

Gibson-Lo Model

The Gibson-Lo model provides a prediction of the one-dimensional compression of soils. This model is stated in the following equation from Edil & Simon-Gilles (1986):

$$\epsilon(t) = \Delta\sigma \left[a + b \left(1 - e^{-\left(\frac{\lambda}{b}\right)t} \right) \right] \quad (2.1)$$

where: $\epsilon(t)$ = strain at time t

$\Delta\sigma$ = applied stress increment

a = primary compressibility

b = secondary compressibility

$\frac{\lambda}{b}$ = rate factor for secondary compressibility

A method presented by Lo, Bozozuk and Law (1976) allows for simple determination of the parameters a , b , and $\frac{\lambda}{b}$. Using this method, the logarithm of strain rate is plotted versus time. The straight line portion of this curve corresponds to the time range of secondary compression. If the straight line is extended back to the y-axis, the parameters can be found by solving simultaneously the following equations:

$$\text{line slope} = 0.434 \left(\frac{\lambda}{b} \right) \quad (2.2)$$

$$\text{y-intercept} = \log(\Delta\sigma \cdot \lambda) \quad (2.3)$$

$$a = \frac{\epsilon_f}{\Delta\sigma} - b + be^{-\left(\frac{\lambda}{b}\right)t_f} \quad (2.4)$$

where ϵ_f = last strain reading

t_f = time of last strain reading

Edil & Mochtar (1984) recommend using linear regression during the time range corresponding to secondary compression. This will tend to reduce the variation of the strain rate resulting from the use of unequal time intervals.

The three parameters a , b , and $\frac{\lambda}{b}$ obtained from laboratory tests are somewhat dependent on the value of stress increment, final stress level, and the average strain rate. Stress increments less than approximately two times the stress level tested in the laboratory will cause little variation in the value of the parameters. However, this is true only for laboratory conditions. The parameters obtained from the analysis of field and laboratory performances are different as a result of the discrepancies between these conditions.

During research conducted by Edil & Mochtar (1984), the laboratory and field behaviors of organic soils under loading were observed. The results were compared to determine any existing relationships between the two conditions. From this comparison they were able to develop correlations between the model parameters for laboratory and field

performance. Figure 2.1 provides a curve of consolidation stress versus primary compressibility. Data points are from laboratory tests and from field observations as distinguished in the figure. The figure indicates that the primary compressibilities in the field and the laboratory are comparable for the same stress level. Therefore, the laboratory value of the parameter "a" will compare with the field value when the variation of soil properties is considered. In addition, the curve fitted through the plotted points can be used to correct the value of the parameter "a" when a prediction is desired at a different stress level.

Figure 2.2 provides a curve of the secondary compressibility factor, "b", versus stress level. The points plotted are for peat data only. As illustrated in this figure, the field value of "b" is higher than the laboratory value at equivalent stress levels. Using Figure 2.2, a plot of $\frac{b_{\text{field}}}{b_{\text{lab}}}$ versus consolidation stress was constructed as illustrated in Figure 2.3. Once again, it should be noted that Figure 2.3 represents data from observations made on peat only.

A plot of strain rate versus $\frac{\lambda}{b}$ is provided in Figure 2.4. This figure indicates that no correlation exists between $(\frac{\lambda}{b})_{\text{lab}}$ and $(\frac{\lambda}{b})_{\text{field}}$.

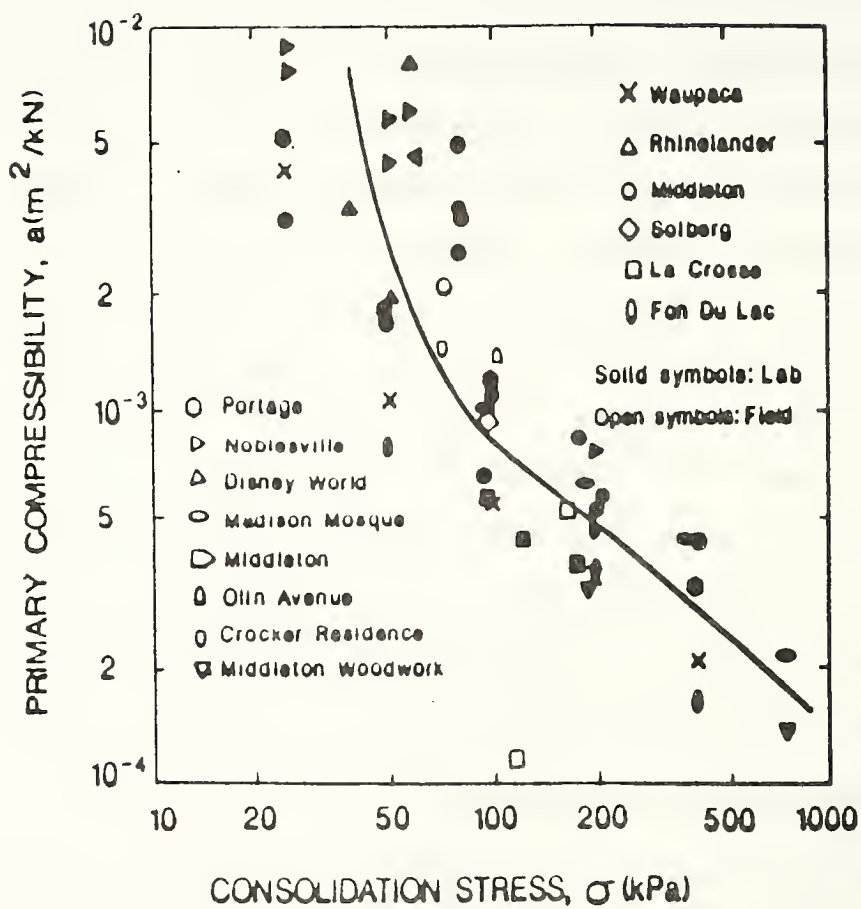


Figure 2.1 Primary Compressibility versus Stress Level. From Edil & Mochtar (1984).

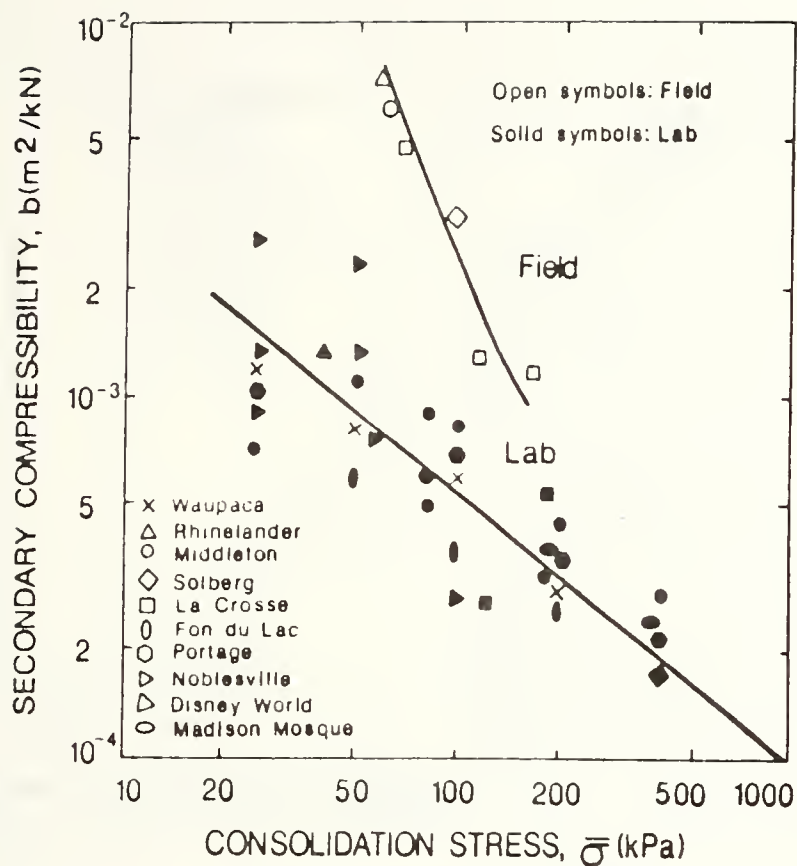


Figure 2.2 Secondary Compressibility versus Stress Level. From Edil & Mochtar (1984).

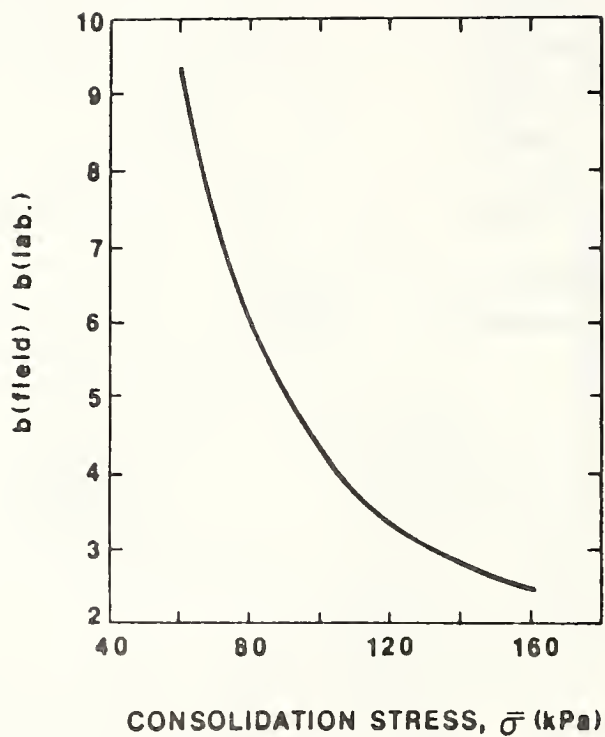


Figure 2.3 Correction Curve for Laboratory Values of Secondary Compressibility. From Edil & Mochtar (1984).

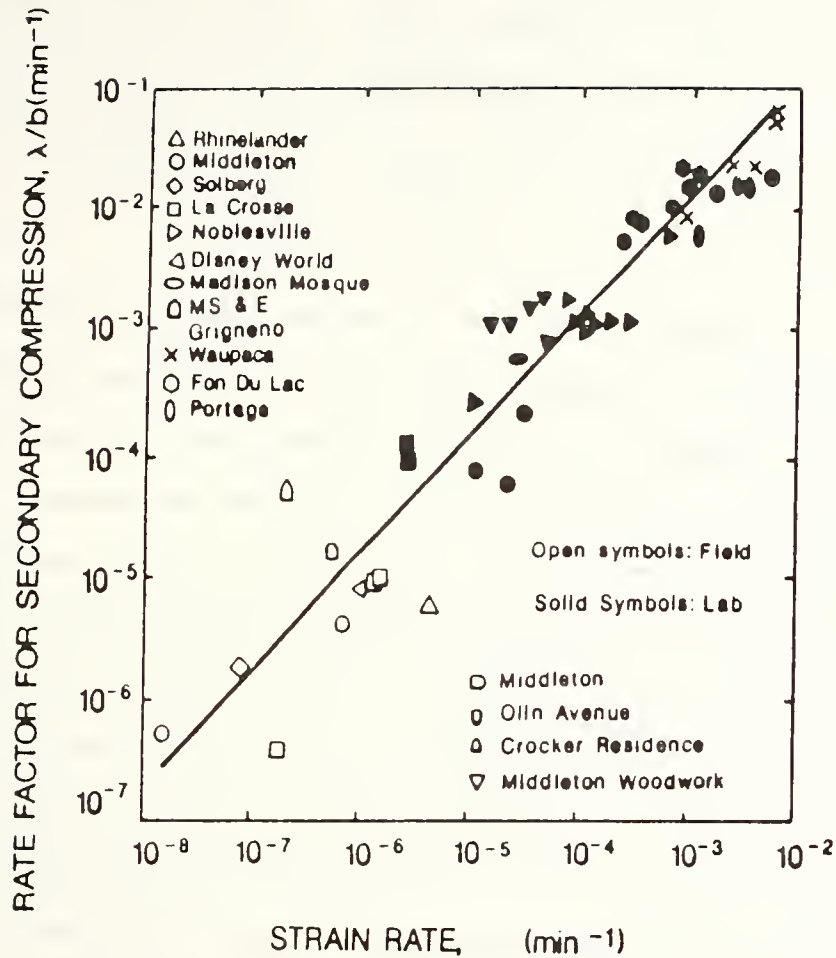


Figure 2.4 Dependency of Rate Factor for Secondary Compression on Average Strain Rate.
 From Edil & Mochtar (1984).

These figures can be used to correct the parameters obtained from laboratory tests for prediction of settlement in the field. Edil & Mochtar (1984) recommend performing the laboratory tests at stress levels that will be applied in the field to eliminate most of the effects of stress level. They also proposed increasing stress levels by amounts that will simulate field loading, rather than using a conventional load-increment ratio.

Once laboratory consolidation tests are conducted in this manner, a curve of log strain rate versus time is constructed and the appropriate parameters are determined. Using Figure 2.3, the value of "b" can be corrected. Figure 2.4 can be used to obtain the $\frac{\lambda}{b}$ (strain rate factor). If the average field strain rate is not known from previous experience, it is recommended that a field strain rate two to three orders of magnitude smaller than that observed in the laboratory be assumed. Using these corrections, Edil & Mochtar (1984) and Edil & Simon-Gilles (1986) were able to predict quite accurately the settlement of peats when loaded in the field.

One of the key assumptions in the development of the Gibson-Lo model is one-dimensional compression. During their study, Edil & Simon-Gilles (1986) noted that inclinometers placed on the sites indicated very small amounts of lateral movement. In this case, the assumption was quite valid.

YIELD ENVELOPE CONCEPT

In research performed by Joseph (1986), K_0 triaxial tests were performed on thoroughly remolded samples of amorphous peat and of muck. The results of these tests indicate that a unique failure envelope in p' - q space exists for amorphous peats and mucks. The observed failure envelope began at the origin and developed concave upwards, indicating that all strength was a result of friction, and that cohesion made no contribution to shear strength. The presence of a unique failure envelope suggests that amorphous peats and mucks fit into the realm of classical soil mechanics, and behavior similar to soft clays can be expected.

The yield envelope concept for soft clays was developed by Tavenas & Leroueil (1977). Joseph (1986) states that the yield envelope concept is valid for amorphous peats and mucks since the consolidation of these materials can be predicted by a generalized consolidation equation.

Watson et al. (1984) provide a synopsis of the yield envelope concept. A diagram illustrating this concept is shown in Figure 2.5. The yield envelope is an envelope of stress states that separates the small strain response to loading from large strain response. The stress value at the point where the yield envelope intersects the K_0 line is approximately equal to the preconsolidation pressure determined in an oedometer test.

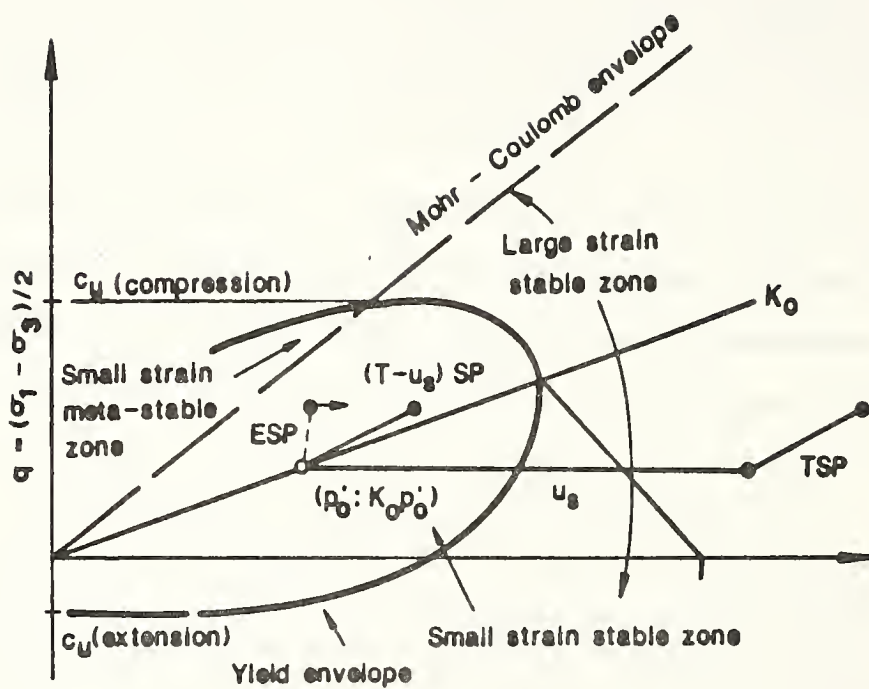


Figure 2.5 Major Features of Yield Envelope.
From Watson et al. (1984).

There are three important phases of soil response that can occur in this diagram, depending upon the effective stress state of the loaded soil. If the effective state of stress remains below the Mohr-Coulomb envelope and is contained within the yield envelope, the soil acts as an over-consolidated material. Upon loading there is a small amount of strain and excess pore pressures dissipate quickly.

If the effective stress state is contained within the yield envelope, but is above the Mohr-Coulomb envelope, the soil is considered to be metastable. If an additional load is placed on the soil causing yield, the effective stress state will move along the Mohr-Coulomb line and strain softening will occur. Strain softening is ordinarily accompanied by an increased amount of pore water pressures, total horizontal stresses, and lateral strains.

The third type of soil response occurs when the effective stress path is situated outside the yield envelope and below the Mohr-Coulomb line. When this condition exists, the soil behaves as a normally consolidated material. Large strains and porewater pressures develop upon loading. The excess pore water pressures dissipate rather slowly.

Watson et al. (1984) suggest that in some instances construction of fills on soft soils should be performed using stage loads. Stage loaded construction allows for a

strength gain to occur in the foundation soil as a result of consolidation when the load is sustained. This strength gain increases stability when subsequent stage loads are applied.

During embankment construction, the extent of lateral deformations should be minimized to reduce the amount of settlement. Watson et. al. (1984) state that by avoiding a stress state causing failure in the foundation material, lateral deformations can be controlled. They suggest constructing the embankment in stages similar to that shown in Figure 2.6. Point E represents the initial state of stress. As the subsoil is loaded, the effective stress path moves along EA' and the total stress path moves along EA.

If at this point construction to the final load is continued, the effective stress path will move along $EA'PR$, and strain softening will occur. Large lateral deformations will develop as a result. However if construction is delayed, the excess pore water pressures will begin to dissipate and the effective stress path will move from A' to A'' in the figure. Once excess pore pressures have dissipated to point A'' , the total load can be increased to total stress state B, which corresponds to effective stress state B' . In this instance, the effective stress path will cross the yield envelope and move into the large-strain-stable zone. Large consolidation settlements will occur in this

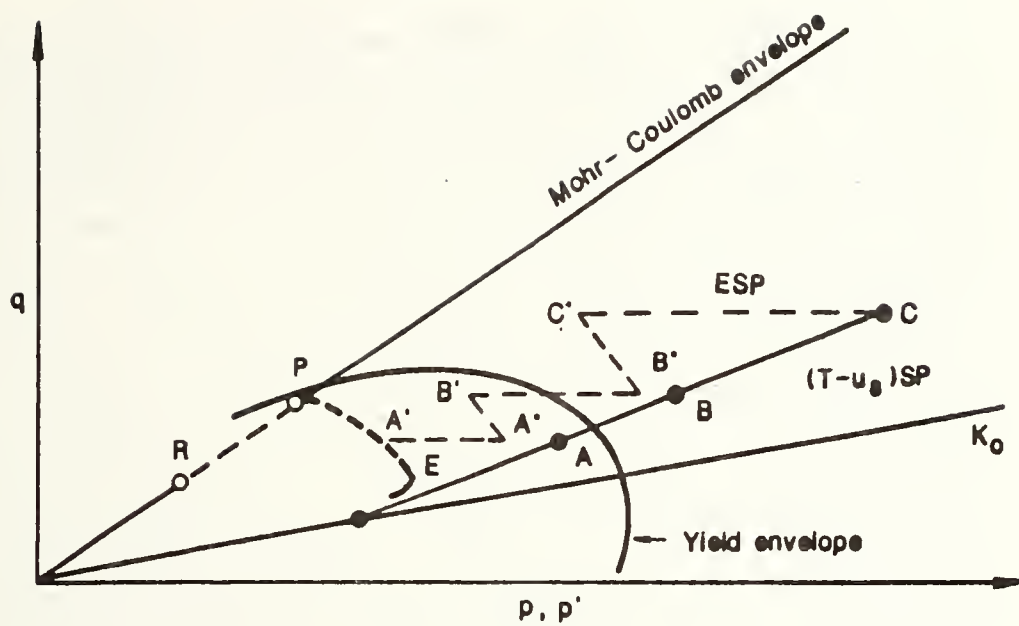


Figure 2.6 Effective Stress Path during Multi-Stage Loading. From Watson et al. (1984).

situation, but positioning of the stress state below the Mohr-Coulomb envelope will keep lateral displacements at a minimum.

CONSTRUCTION TECHNIQUES

Stage Loading

Both Gruen & Lovell (1983) and Joseph (1986) recommend the use of stage loading when constructing embankments over amorphous peats and mucks. The low shear strengths associated with these materials cause stability problems during construction. However, construction in stages, as discussed in the previous section, will allow strength gain while the load is held constant. In this manner the embankment can be constructed to its final height in a number of steps, and stability problems are avoided. In many cases on such soft materials, if the embankment were constructed to its final height in one step, the foundation materials would fail. Staged loading also allows for a large portion of settlement to occur during construction, reducing the amount occurring during the service life of the embankment.

Berms

Joseph (1986) discussed the use of berms during embankment construction. Berms are used to reduce lateral deformation and increase stability of embankments constructed on

soft soils. Raymond (1969) and Hollingshead & Raymond (1971) indicate that berms provide a useful means of reducing undrained movements, therefore limiting the amount of shear deformations. Raymond (1969) suggests that successful use of berms requires that the berm width be $1\frac{1}{2}$ to 2 times the depth of the peat and marl.

Raymond (1969) emphasizes that the extent of the benefit provided by berms is greatly influenced by the sequence of construction. Less shearing stress develops if the embankment is constructed simultaneously from both outer edges inward to the centerline. This method was considered better than construction from the centerline outward or from one side to the other. Construction from the outer edges to the center has the advantage of trapping a developing mud wave in the center. In addition, if construction is performed in this manner, a berm failure is not likely to cause extensive damage beneath the central fill area.

Sand Drains

Joseph (1986) reviewed the use of sand drains to increase the rate of pore pressure dissipation during construction. From his review of literature on this topic, he concluded that sand drains do not provide much help in this manner. However, various researchers believe that sand drains have a beneficial effect on stability as a result of

pile action. Reduced wave action under traffic loads has also been observed when sand drains are in place, indicating they may sustain a portion of the load. Support may be provided in a direct manner by the drains themselves, or in an indirect manner through arching.

Geotextiles

The use of geotextiles during construction of embankments over such soft materials is becoming increasingly popular. Research performed by various investigators indicates that geotextiles provide a number of positive effects when they are used during projects of this nature.

Petrik et al. (1982) performed model tests to determine the behavior of a reinforced embankment. Two reinforcing materials were tested. One material was a polypropylene woven fabric, and the other was a brass sheet. The latter was included to determine the effects of a rigid reinforcing material.

It was concluded from this research that the amount of horizontal deformation is significantly affected by the presence of reinforcement. However, the amount of vertical deformation that occurs is not substantially influenced by the presence of a geotextile. It was also concluded that both the bearing capacity and stability are enhanced through the use of fabrics. Tests performed on the embankment

models reinforced with brass were observed to result in higher bearing capacities, and to produce lesser lateral strain of the foundation material than those reinforced with the polypropylene fabric. These results imply that the stiffer reinforcement mobilized a higher strength in the subsoil.

Hutchins (1982) discussed the behavior of a shallow embankment constructed over a deep black marsh muck with the use of geotextiles. A spunbonded polypropylene geotextile was placed on the muck surface, and a granular embankment fill was subsequently constructed. After construction, three types of plate load tests were performed at the site. The first type of test consisted of excavating a small hole in the embankment to the muck level. A plate load test was then performed directly on the fabric. The second type of test also consisted of excavating a hole to the muck level, however the geotextile was cut, and the plate load test was performed directly on the muck. The third type of test was performed on the in situ soil, away from the embankment.

The results of this testing indicate that the effective bearing capacity under the geotextile increased by 39% at failure. The increase in bearing capacity was attributed to a modulus or membrane effect provided by the geotextile.

During construction, a portion of the embankment was placed without the use of a geotextile. In this section the

contractor used twice the volume of sand to attain the same elevation as the section with the fabric. Hutchins (1982) theorized that the extra sand was used in the areas of local shear failure. The extra fill required in this section was a result of a lower modulus of subgrade reaction, K_s , and an irregular cross-section of the embankment.

Hutchins (1982) cites bridging over weak areas as another advantage of the use of geotextiles. During site investigation, areas of low bearing capacity will be missed even during the most thorough investigations. Previously, engineers have designed embankments with a factor to account for these weak areas. However, this is not an economical design procedure. If geotextiles are placed in the embankment, they help to bridge the embankment over such areas, eliminating the need for overdesign for this criterion.

Barsvary et al. (1982) also studied field performance of a highway embankment constructed over an amorphous granular peat underlain by sands and a soft to stiff clay. A beneficial result of the use of geotextiles during this project was the formation of a barrier between the foundation and embankment materials. Barsvary et al. felt that the barrier reduced the problem of stability which is aggravated when the two materials intermix.

To determine that the geotextile truly does provide an adequate barrier, excavations were made through the fill one

year after construction. There was no mixing of the subgrade with the embankment where geotextiles were used. However, in areas where no geotextiles were used, an irregular interface developed between subgrade and fill materials and the two soil types were intermixed.

During construction of the embankment over this peat, the first stage was completed without any sign of rotational failure. Barsvary et al. believe that the membrane effect provided by the geotextile prevented such a failure. Strains of 2 to 5 percent were observed in the transverse and longitudinal directions at this point. The fact that strains developed in the longitudinal direction implies that plane strain conditions may not be an accurate assumption under low embankments constructed on highly compressible soils. This is the result of inconsistencies of the foundation material such as soft areas and tree stumps.

During the second stage of construction, the longitudinal strain was 8 percent at the center of the fill, while transverse strain approached failure. Some mud waves and tension cracks were observed to develop near the embankment toe, indicating that there was deformation in lateral shear. Although there was evidence of lateral deformation, there were no tension cracks or horizontal displacements observed in the embankment. The geotextile is credited with restraining the embankment and preventing any lateral spreading from occurring.

Hannon (1982) observed the performance of a test embankment constructed over San Francisco Bay Mud with geotextile reinforcement. The embankment was constructed to a height of 16 feet prior to settlement with a planned final height of approximately 10-12 feet. During one year, approximately 6 1/2 feet of settlement occurred. Wick drains were installed to accelerate consolidation.

During construction of the embankment, high excess pore pressures developed, which the author felt were capable of causing a shear failure. Hannon (1982) believed that the geotextile was responsible for the successful construction of the embankment without incurring any failures. In an adjacent area, the embankment was constructed by end dumping without the use of sand wicks or fabrics. In this instance, construction resulted in the development of a large mudwave.

As a result of loading from truck wheels during construction, approximately six inches of instantaneous compression were observed. The reaction was quite similar to that of a large waterbed. Hannon (1982) believed that the geotextile contributed to stability and kept the embankment intact. Over a three month period, three inches of lateral displacement were observed. However, in such a soft foundation material this is not considered to be a significant amount.

Research conducted by Boutrup & Holtz (1983) used the finite element method to analyze the effects of geotextiles on embankment behavior. A portion of their investigation focused on determining the benefits of placing geotextiles higher up in the embankment between lifts. A finite element analysis performed with three layers of fabric placed between lifts resulted in a maximum reduction in shear stresses of 13%. However, an analysis performed with one layer of fabric placed at the interface between the embankment and foundation materials resulted in an 11% reduction of shear stresses. It can be seen from this comparison that the benefit of multiple layers of geotextile is not significant.

An analysis was also performed to determine the effects of the placement of two layers of geotextile between the embankment and the foundation. The results indicated an 18% reduction in maximum shear stress. One layer of geotextile possessing twice the modulus will produce the same results. Therefore, the use of this procedure is more effective than the use of multiple layers of geotextiles.

Humphrey (1986) investigated the use of the cap soil behavior model in a plain strain finite element analysis. The cap model is a nonlinear elastic-plastic isotropic work-hardening plasticity model. A drawback of this model is the absence of a method to reliably determine the

required model parameters from conventional test results. Humphrey presents a method that allows for simple parameter determination. The main input soil parameters required are the compressibilities in virgin loading and unloading/reloading, the effective Mohr-Coulomb shear strength parameters (ϕ' and c'), and the undrained shear strength ratio s_u/σ'_p .

A weakness of the analysis using the cap model is its inability to predict behavior when the principal stresses rotate 90 degrees. As a result of this, Humphrey recommends using finite element analysis only for an estimation of forces in the geotextile when the foundation fails, or to make a comparison between reinforced and unreinforced embankment behavior. Limit equilibrium analysis should be used during design to determine the factor of safety against various failure modes. For a more indepth discussion of the design of reinforced embankments, the reader should consult both Humphrey (1986) and Boutrup & Holtz (1983).

CHAPTER III-TESTING PROGRAM

INTRODUCTION

A critically important portion of this research includes the development and implementation of a soil testing program to determine various parameters required for design and construction of embankments over amorphous peats and mucks. This chapter will provide a discussion of the materials tested during the project and give a description of their behavior. Also covered will be the preparation of samples for laboratory testing, as well as procedures and results of creep tests, K_0 triaxial tests, and field vane shear tests. During K_0 triaxial testing, a major equipment modification was necessary, and a description of this device, as well as other required equipment not commonly found in geotechnical laboratories, will be provided.

MATERIALS STUDIED

The laboratory behavior of both an amorphous peat and a muck were studied during this research project. The amorphous peat was obtained from a portion of the shoreline of Otterbein Lake in Benton County, Indiana. The muck was sampled from a depression along a portion of Lindberg Road in West Lafayette, Indiana.

Disturbed samples of these materials were obtained from these sites using shovels. Samples were placed in 10 gallon containers which were sealed with airtight lids. Sufficient water from the site was placed in the containers to keep the materials saturated in natural waters during storage.

Laboratory tests were performed to determine the specific gravity, organic content, liquid limit and plastic limit of each material, as described in ASTM Standard Specifications D854-83, D2974-84, and D4318-84 respectively. A tabulation of these characteristics, as well as other values previously determined by Joseph (1986) appears as Table 3.1. Asterisks indicate values taken from Joseph.

PRODUCTION OF SAMPLES FOR LABORATORY TESTING

As stated in the previous section, the samples were obtained from disturbed sampling at the site. Samples were obtained by this means as a result of the decision to perform tests on thoroughly remolded samples prepared from a slurry. This decision was based on the fact that it is very difficult to obtain an undisturbed sample of these materials suitable for triaxial testing. The low preconsolidation pressures typical of these materials makes them soft, and trimming of samples would result in a large amount of disturbance from handling. Also, for triaxial testing a membrane must be placed over the sample. This process would

Table 3.1 Soil Characteristics

QUANTITY	OTTERBEIN LAKE	LINDBERG ROAD
Specific Gravity	1.8-2.0	2.2-2.5
Organic Content	55.3%	34.7%
Liquid Limit	**	123.5%
Plastic Limit	**	92.2%
Water Content	365-465 *	130-140 *
pH	6.75 *	6.5 *
Initial Void Ratio	10-21 *	2.9-4.7 *
Fiber Content	Nil	Nil

* Indicates values taken from Joseph (1986)

** Atterberg Limits could not be tested for this material as a result of the lack of cohesion.

seriously disturb the sample. Production of samples from a slurry has the advantage of allowing the sample to be formed inside a membrane for triaxial tests, which greatly reduces the amount of handling.

In research conducted by Landva (1986) the validity of the use of remolded slurry samples for fibrous peats was investigated. When the results of tests performed on undisturbed samples and remolded samples were compared, nearly identical shear and consolidation properties were observed. Landva (1986) concluded that the fabrics of undisturbed samples and remolded samples were quite similar after consolidation under initial loads.

Before producing a slurry, the appropriate water content must be decided upon. Krizek & Sheeran (1970) present factors to consider before choosing a water content. They state that a high water content slurry has the advantages of being easily deaired and more easily placed in the consolidometer. In addition, the method of placement in the consolidometer has less influence on the fabric of the sample. However, the disadvantages of a high water content are segregation of soil particles in the slurry and a longer amount of time required to consolidate the sample. Krizek & Sheeran (1970) recommend determining the best water content by trial and error, using 1.5 to 2 times the liquid limit as a starting point.

During this project, a water content of approximately 1.5 times the liquid limit was chosen for the muck. Atterberg limits could not be tested for the amorphous peat as a result of the lack of cohesion. Therefore, the minimum water content providing a workable slurry was chosen by trial and error.

Once the slurry water content was determined, slurry production could begin. The appropriate amounts of soil and distilled water were obtained and placed in a blender. The blades of the blender were covered with a few layers of masking tape to prevent damage to the individual soil particles. When the mixture appeared to be uniform, the slurry was removed from the blender and placed in a deairing chamber for 24 hours or until the level of the slurry was not observed to decrease when the vacuum was released. After deairing, the slurry was poured into the consolidometer and the appropriate consolidation pressure was applied.

The consolidometer present in the laboratory is shown in Figure 3.1. This equipment allows samples to be consolidated within a membrane. Originally this consolidometer was designed for use in a loading frame where the consolidation pressure was applied through a load cell. However, the loading frame present in the laboratory was being used quite steadily for another project. To overcome this, an inexpensive clamp was constructed to hold the piston in place.

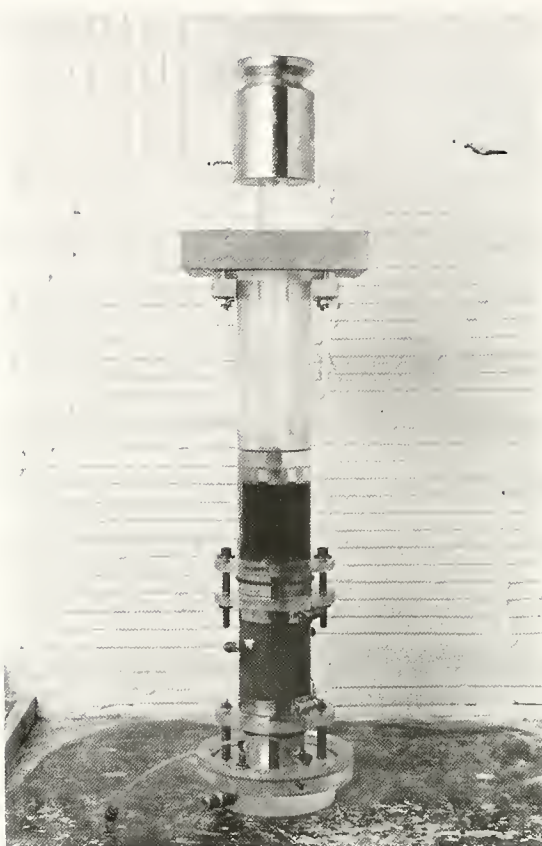


Figure 3.1 Slurry Consolidometer.

Since consolidation loads required to produce samples were low, dead weights were placed directly on the piston to eliminate the need for a loading frame and load cell.

There was no existing equipment in the laboratory for production of samples for creep tests. A modification of the consolidometer was developed to allow consolidation of the slurry to occur in the oedometer ring to reduce handling of the sample. A photograph of this modification is shown in Figure 3.2.

CREEP TESTING

Samples were produced from a slurry in the oedometer ring at pressures of 0.7 psi, 3.0 psi and 6.0 psi. Once samples were consolidated, the excess material was trimmed away to form a sample with a thickness of one inch. The weights of the oedometer ring and sample were recorded for each test. The oedometer cell was then assembled and placed on the loading frame. To eliminate the effect of temperature variation on the creep test results, the loading frame was surrounded by insulated panels. Samples were backpressure saturated for approximately 48 hours, beginning at 10 psi and increasing the pressure to 40 psi in increments of 10 psi.

Samples were then reloaded to the consolidation pressure at which they were formed in the consolidometer. Once

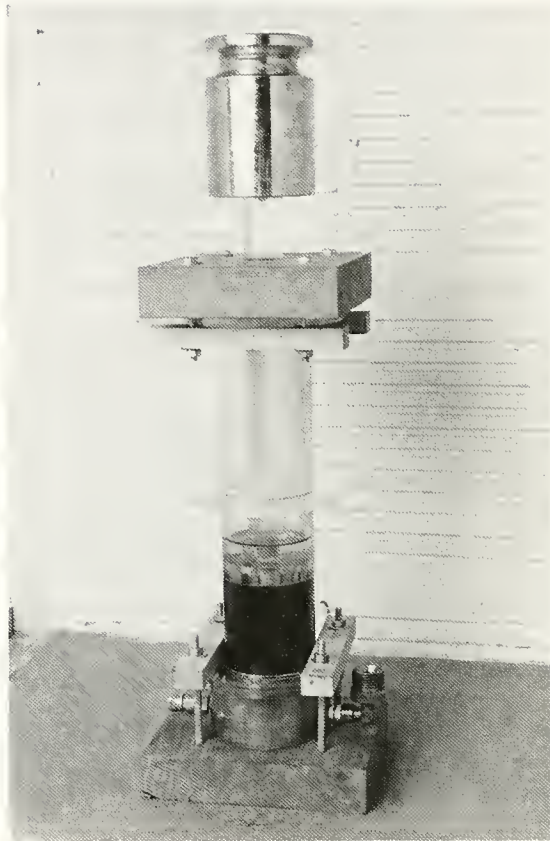


Figure 3.2 Slurry Consolidometer Adapted for Production of Creep Test Samples.

secondary compression was observed, the loads on the samples consolidated to 0.7 psi, 3.0 psi, and 6.0 psi were increased to 3.0, 6.0, and 9.0 psi respectively. Two tests were also conducted by increasing the load from 0.7 psi to 9.0 psi to simulate construction of the entire embankment. Loading was sustained on each sample until sufficient data of secondary compression had been collected for determination of the modified coefficient of secondary compression, C_{α_e} .

Typical test results for each material are provided in plots of strain versus log time in Figures 3.3 and 3.4. The remaining test results are provided in Appendix A. Test materials and consolidation pressures are signified in the following identification scheme. Samples from Otterbein Lake are represented by OL and samples from Lindberg Road are identified by LR. The number following these symbols indicates the final consolidation stress of the test. The second number indicates the number of the test performed at that stress level. Therefore, OL-6-1 identifies the first test performed on samples from Otterbein Lake consolidated at 6 psi. Tests OL-9-2 and LR-9-2 represent tests on samples formed at 0.7 psi and consolidated at 9.0 psi.

The values of C_{α_e} were calculated for each test as illustrated in Figure 3.5. The resulting values are shown in Table 3.2. It should be noted that tertiary compression

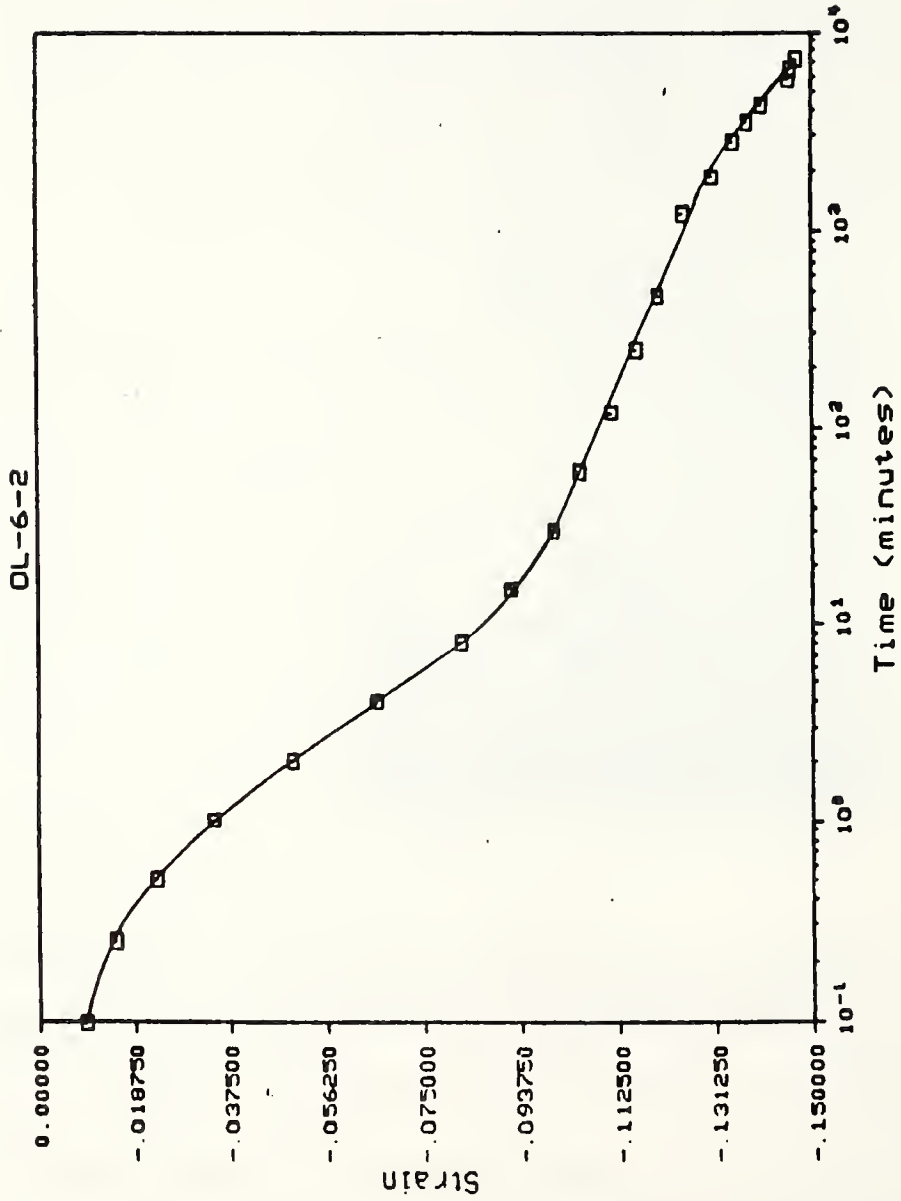


Figure 3.3 Strain versus Logarithm Time, Creep Test OL-6-2.

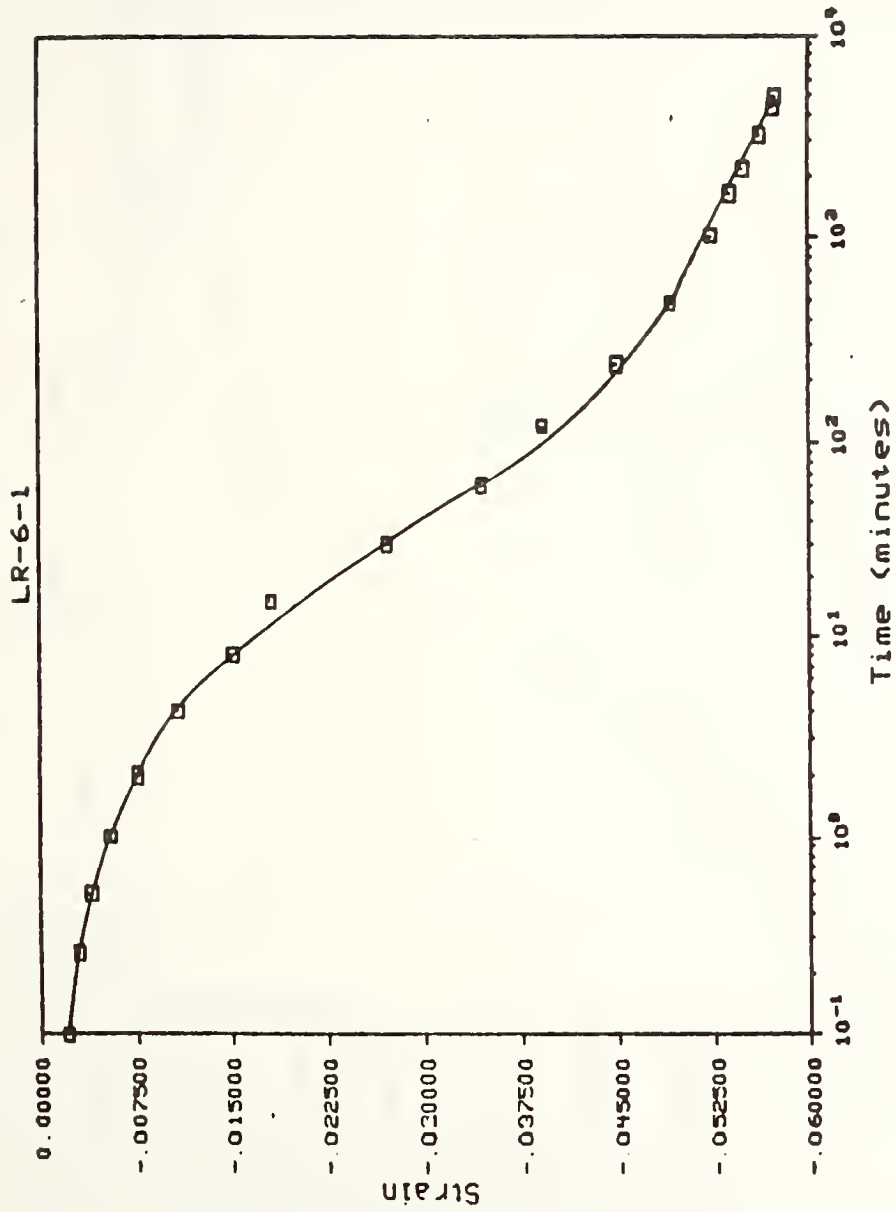


Figure 3.4 Strain versus Logarithm Time, Creep Test LR-6-1.

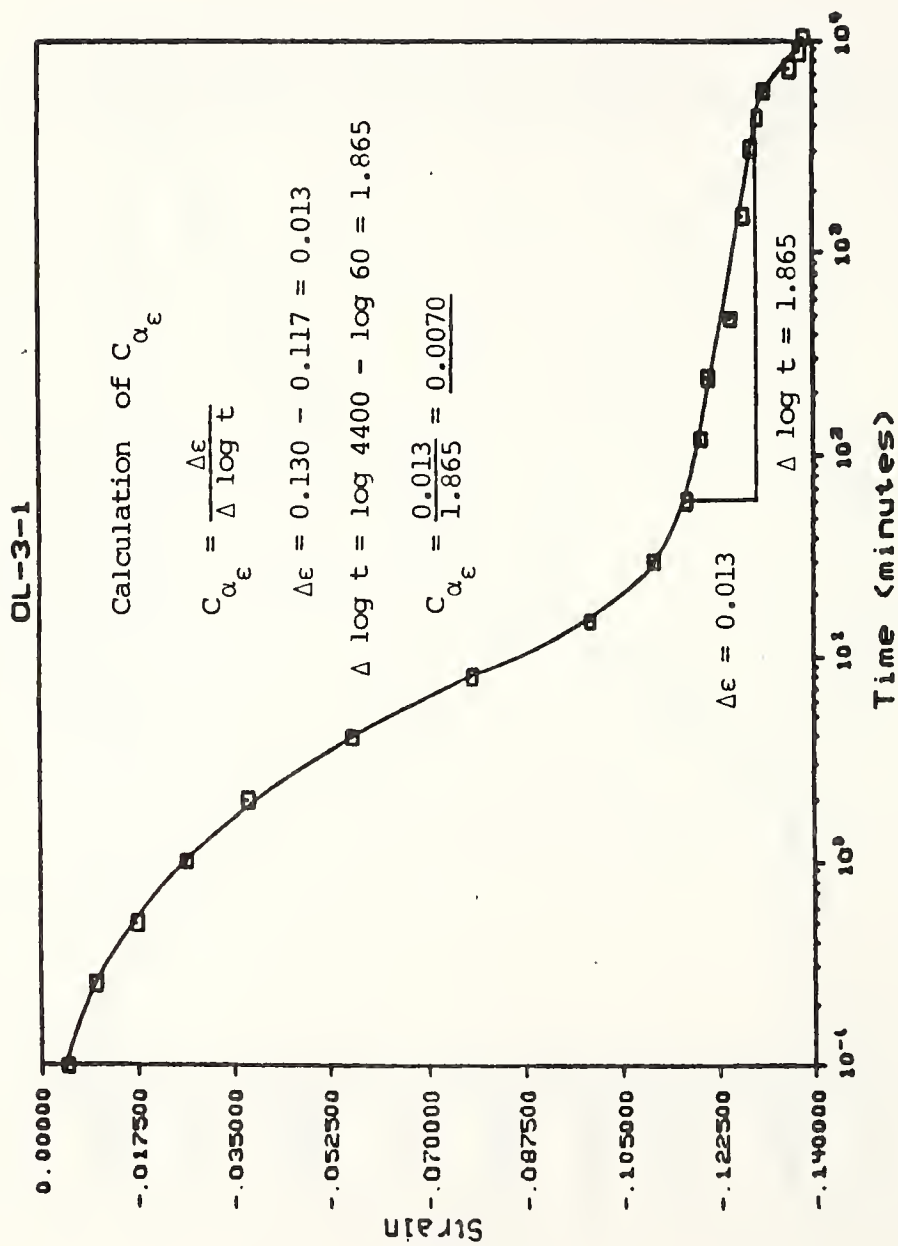


Figure 3.5 Calculation of C_{α_E} .

Table 3.2 Values of C_{α_ϵ}

TEST NO.	C_{α_ϵ}
OL-3-1	0.0070
OL-6-1	0.0184
OL-6-2	0.0167
OL-9-1	0.0298
OL-9-2	0.0171
LR-3-1	0.0086
LR-6-1	0.0083
LR-6-2	0.0105
LR-9-1	0.0247
LR-9-2	0.0135

was observed in tests performed on the peat samples from Otterbein Lake. This was expected as this material was a peat. As previously mentioned, Edil & Simon-Gilles (1986) state that although tertiary compression has been observed in the laboratory, they have no evidence of such occurrence in the field. However, it is possible that it does occur under field loading conditions, but is masked by other settlement phenomena occurring at the same time.

K_0 TRIAXIAL TESTING

The second portion of the testing program consisted of performing K_0 triaxial tests. Gruen & Lovell (1983) state that construction of embankments over peat deposits results in deformations resembling those in axial compression. K_0 conditions were chosen for a number of reasons. For a long narrow loading such as an embankment, deformations are assumed to be negligible in the direction of the embankment axis. Deformation would therefore only occur in the direction perpendicular to the embankment centerline. It was felt that K_0 conditions would be a much better approximation of this behavior than isotropic conditions. Also, according to Lambe & Whitman (1979), if two samples are consolidated to the same vertical effective stress, one isotropically and one under K_0 conditions, the K_0 consolidated sample will possess a lower undrained shear strength. Therefore, K_0 conditions were chosen as they provide a conservative estimate of the undrained shear strength.

It is the aim of the construction method to be developed later in this report to construct embankments over these materials with reduced lateral deformations. This is essential as the Gibson-Lo Model for settlement prediction does not account for shear deformations. K_0 conditions therefore represent most closely the anticipated loading of the subsoil.

The principle of K_0 triaxial testing requires the prevention of change in cell water volume during consolidation, preventing lateral expansion of the sample. This is accomplished with the use of equipment developed by Campanella & Vaid (1972). They developed equipment utilizing a Bellofram piston with the same diameter as the soil sample. During consolidation the cell valve is closed to keep the volume of cell water constant. As the sample consolidates, the sample volume lost from compression is replaced by the piston as it advances into the cell.

Problems were encountered with the use of this equipment on soft materials such as amorphous peats and mucks. The Bellofram piston in the existing equipment provided only $1 \frac{1}{2}$ inches of stroke, which was not sufficient to consolidate and shear samples. In an attempt to alleviate this problem, the sample height was reduced from 6 inches to 5 inches, and the pedestal was elevated one inch to accommodate this change. The modification was attempted on the basis

that for the same percentage of strain required to complete the tests a lesser amount of vertical deformation would be required. This adjustment did not provide the necessary amount of correction.

Since Bellofram does not manufacture a $2 \frac{1}{2}$ inch diameter piston with sufficient stroke, a new piece of equipment had to be developed. The solution was to construct a system using a linear bearing to allow movement of a $2 \frac{1}{2}$ inch diameter piston to replace the need for the Bellofram. The design is similar to that of an oedometer cell. As with the oedometer, an O-ring is placed beneath the bearing on the inside of the cylinder to prevent leakage of water into the bearing.

The weight of a solid steel piston would result in excessive loads being placed on the samples. It was therefore decided to use a hollow aluminum piston to reduce the weight. The aluminum tube was anodized to harden it sufficiently to prevent damage as it moved through the linear bearing. However, when the anodized aluminum was run through the bearing, the piston jammed and streaks developed in the piston walls. It was later determined that even though the piston surface was anodized, the aluminum beneath the surface was still soft, allowing indentations to develop which jammed the system.

At this point there was no option but to use a case-hardened steel piston. To counteract the excessive piston weight, a counterbalance system was developed. Photographs of the redesigned linear bearing system are shown in Figures 3.6 and 3.7, while the counterbalance system is detailed in Figure 3.8.

Once the counterbalance system was constructed, the weight required to balance the piston had to be determined. It was not necessary to counterbalance the entire piston weight as there was some friction in the system at the interface between the piston and the O-ring. The piston was also partially supported by the buoyant force of the water. The counterbalance weight was determined by attaching containers of water to the cable pulley system. Equal amounts of water were added to each container until the piston was no longer observed to descend under its own weight.

During the first test performed with this equipment, a large amount of resistance was observed when the cell pressure was raised to large values. It is hypothesized that the high cell pressures exerted on the O-ring caused it to tighten around the piston as a result of the Poisson's ratio. To reduce friction, the lubricant used on the piston was changed from silicon oil to automotive grease. Lubri-Matic Multi-Service Lubricating Grease, available at Sear's Automotive Departments, was chosen for its high shear

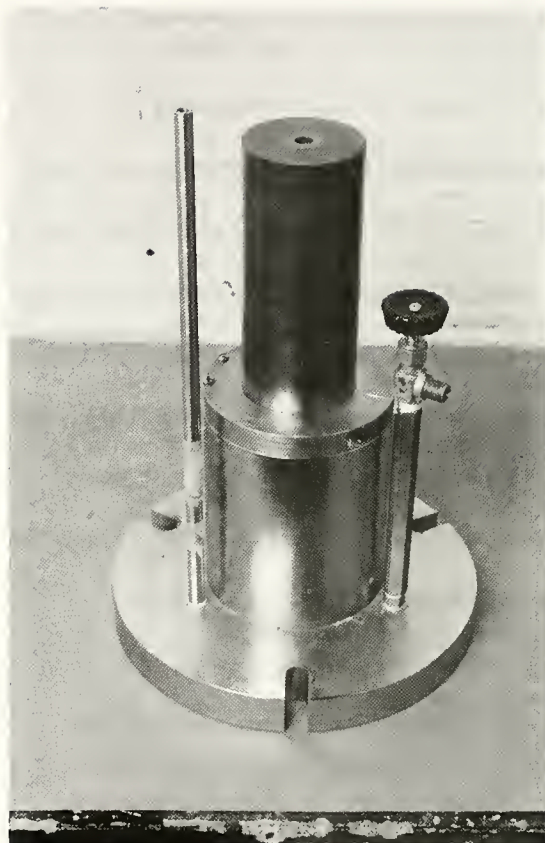


Figure 3.6 New K₀ Triaxial Cap, Top View.



Figure 3.7 New K_0 Triaxial Cap, Bottom View.

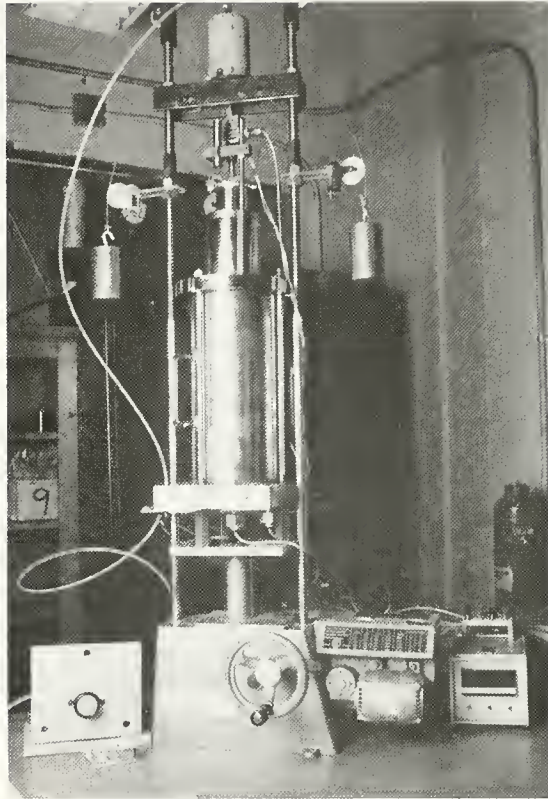


Figure 3.8 K_0 Triaxial Apparatus.

stability and water resistance. The increased resistance was also caused in part by uplift forces, as the diameter of the top platen was slightly less than that of the piston. The piston was then calibrated for resistance at high pressures, which was subsequently determined to be approximately 1 psi.

Samples were produced from a slurry in the consolidometer at a pressure of 3.0 psi. After the samples were consolidated, the excess material was trimmed to form a sample with a height of 6 inches. The samples were then carefully mounted on the base pedestal. Once the plastic former was removed from the samples, great care was taken not to vibrate the apparatus, as the vibrations were observed to cause the soft samples to slough.

After the samples were installed, backpressure saturation began. Cell pressure was constantly kept 1 psi higher than backpressure to prevent ballooning of the membrane. Using the control panel, cell pressure and backpressure could be increased simultaneously, but the axial pressure on the piston had to be increased separately. To avoid damaging the sample with large stress differences, the cell pressure/backpressure and axial pressure were increased in steps of 1 psi. If larger increments were used, the sample was observed to deform as a result of differences between axial and radial pressures. The samples were backpressure saturated to 80 psi. A high cell pressure was desired to

reduce the compressibility of water under additional stresses. This is necessary to keep the cell volume constant during K_0 consolidation.

Once the samples were saturated, they were consolidated under K_0 conditions. Samples were consolidated at twice their preconsolidation pressures to reduce the effects of disturbance from handling. Therefore, samples formed from the slurry at 3.0 psi were consolidated at 6.0 psi. The samples were allowed to consolidate until secondary compression was observed. At this point, the samples were loaded axially until shear failure occurred. A step by step listing of the procedure for K_0 triaxial tests including installation, saturation, consolidation, and axial loading is provided in Appendix B. The results of K_0 triaxial testing are presented in Table 3.3.

FIELD VANE SHEAR TESTS

When the results of K_0 triaxial tests were used in design analyses, a number of problems developed. Based on the conclusion of Joseph (1986) that a linear strength line exists from 0 to 30 psi, it was assumed that the value of s_u/σ'_p would be constant. However, it was later observed that Joseph's testing program was performed at stress levels equal to or greater than 15 psi, and that the linear strength line was an extrapolation. Thus, the assumption of

Table 3.3. K_o Triaxial Test Results

TEST NO.	K_o	s_u (psi)
S-OL-6-1	0.384	2.21
S-OL-6-2	0.408	2.18
S-OL-6-3	0.321	2.76

a constant value of s_u/σ_p' initially made during this project was not sound.

The only method of finding the shear strength at lower stress levels was to perform the tests at the preconsolidation pressures to be encountered in the field for direct measurement of the undrained shear strength. However, the low stress levels often associated with deposits of this nature made triaxial testing at these levels very difficult. Samples formed at pressures required to simulate field conditions would be too soft, and would not be able to support themselves once the top platen was placed.

The analysis of strength gain beneath the embankment as a result of consolidation was found to be cumbersome. Approximations had to be used to determine the extent of consolidation beneath the embankment. More difficulty was encountered when attempts were made to find the extent of consolidation adjacent to the embankment. A large amount of strength gain adjacent to the embankment is a result of horizontal consolidation, and this effect is difficult to estimate.

In addition to technical problems, the recommendation of K_0 triaxial testing was also impractical on the basis of economics. The equipment required for K_0 triaxial tests, and the production of remolded samples, is not commonly

found in geotechnical engineering laboratories. These pieces of equipment would need to be custom made, and would be very costly. Also, a large amount of time is involved in the production of samples and the testing itself.

In view of these facts, it was felt that the use of the field vane shear test to determine the undrained shear strength was much more practical. Field vane shear tests provide a more expedient method of data acquisition. By measuring directly the values of undrained shear strength both beneath and adjacent to the embankment, this method eliminates the need for assumptions regarding the effects of consolidation within the foundation. The equipment required for such tests is readily available and inexpensive.

Field vane shear tests were subsequently performed at Otterbein Lake using the procedure outlined in ASTM Standard Specifications D2573-72. Tests were conducted using a $2\frac{1}{2}$ inch diameter vane. The values of undrained shear strength obtained from vane shear testing are presented in Table 3.4.

According to Bjerrum (1972), the results of field vane shear tests are dependent upon the rate of loading, soil anisotropy, and progressive failure. When clays are loaded, the shear strength is observed to increase with the rate of loading. A clay which is failed within a few minutes can exhibit values of undrained shear strength considerably

Table 3.4 Values of Undrained Shear Strength from
Field Vane Shear Tests

TEST NO.	DEPTH (FT)	SHEAR STRENGTH (PSF)
1	1.5	384.0
2	1.5	345.6
3	1.5	371.2
4	5.0	332.8

greater than the strength that would be mobilized over a longer period in the field.

As a result of the rate effect, the factors of safety of failed embankments back-calculated from the results of field vane shear tests indicated that in general the vane test overestimates the actual strength. The amount of overestimation increased with the plasticity index of the soil. In order to overcome this, Bjerrum et al. (1972) presented the correction illustrated in Figure 3.9. The results of field vane shear tests should be multiplied by the appropriate correction factor for use in design analyses.

During this research, the results of these tests performed on the amorphous peat were not corrected. This material was non-plastic, resulting in a correction factor larger than one. It was felt that such a correction would be unconservative.

The undrained shear strength of normally consolidated clays is dependent upon the direction in which shear occurs, indicating that the results of field vane shear tests are affected by soil anisotropy. However, when the results of triaxial compression tests, triaxial extension tests, and direct shear tests were averaged and compared with the results of field vane shear tests, a reasonable agreement was observed. As a result, it was concluded that the vane

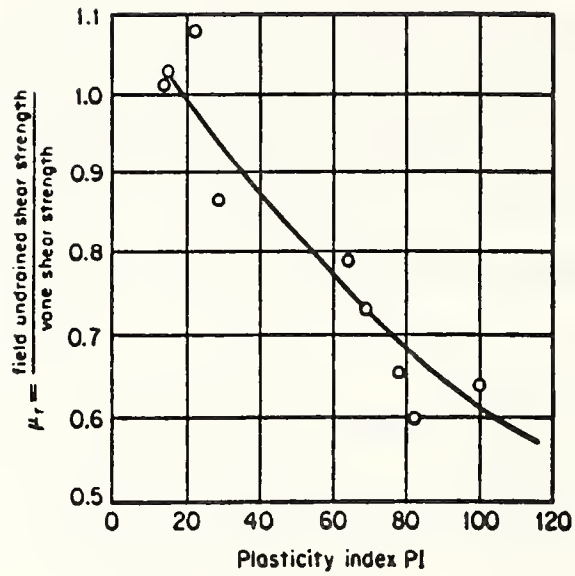


Figure 3.9. Loading Time-Rate Correction Factor versus Plasticity Index for Undrained Shear Strength as Measured by the Field Vane. From Bjerrum et al. (1972).

shear strength could be considered representative of the average shear strength along the slip surface.

In some instances, soft clays possess stress-strain curves with a sharp peak, followed by a substantial loss of shear strength occurring after failure. When a clay fails, the peak shear strength will be mobilized simultaneously at all points only if the strains are uniform. However, this is not the ordinary response.

The failure will initiate in the most severely stressed zones beneath the embankment, and gradually progress into the lesser stressed zones at the embankment sides. Once sliding occurs over the entire failure surface, the soil beneath the loaded area has been strained beyond the peak. If a strain-softening material exists, the results of field vane shear tests will overestimate the resistance of the deposit at failure. For such materials, vane shear testing should include measurement of the remolded strength, as described in ASTM Standard Specification D2573-72.

These limitations should be considered when interpreting field vane shear tests for use in design analyses. It should also be noted that it was assumed that the behavior of amorphous peats and mucks is similar to that of soft clay, and that the use of field vane shear testing in the above manner is applicable to these materials as well.

Since vane shear test data in peats are scarce, further verification of this assumption is recommended.

CHAPTER IV-PROCEDURE FOR DESIGN AND CONSTRUCTION

This chapter provides a complete step-by-step procedure to accomplish the stated objective. Numerical examples are given in Appendix D.

SITE EXPLORATION

An important step in determining the behavior of embankments over amorphous peat or muck is the obtaining of reasonable soil parameters for analysis. However, before these parameters can be established, representative soil characteristics of the deposits must be determined. This is not an easy task when dealing with materials of this nature.

Difficulty in finding representative characteristics of the deposits is the result of the variability typical of amorphous peats and mucks. In order to find the range of existing soil conditions at the site, a preliminary soil survey should be conducted. Disturbed samples may be taken at various depths using a hand auger or a power auger. Samples obtained in this manner may be used for the determination of water content, organic content, and specific gravity. As the compressibility and preconsolidation pressure of the soil throughout the deposit are also needed, creep tests should be performed on undisturbed samples. Field vane shear tests should be conducted throughout the site at various depths to determine the undrained shear strength.

The most critical value to be measured during the site investigation is the undrained shear strength. The value that the designer selects must be conservative as a result of the low factors of safety used in design. For projects such as earth-dams, Terzaghi & Peck (1967) recommend spacing borings at a maximum of 100 feet. The variability of deposits of amorphous peat and muck requires more extensive testing. For the purposes of this thesis, a spacing of not greater than 25 feet along the embankment centerline is recommended. Tests should be performed near the surface, at mid-depth, and near the bottom of the deposit, in order to obtain sufficient information regarding the strength profile.

The results of the preliminary investigation should be used to locate the poorest conditions at the site. If possible, the roadway should be realigned to avoid this area.

During site investigation, the depth of the amorphous peat or muck in the region of the proposed embankment must be determined. A procedure for estimating the thickness of peat deposits is provided in ASTM Standard Specification D4544-86. This procedure uses graduated steel rods of 9.5 ± 1.0 mm diameter and 1.0 or 1.2 m length. The rods can be threaded together to allow use in deposits of any reasonable thickness. Testing involves pushing or driving the rod into the deposit until the resistance to penetration is observed

to increase sharply. This depth of increased resistance should be recorded as the deposit thickness. If sampling is desired, a piston-type sampling device as described in MacFarlane (1969) can be attached to the rod assembly. This method has a number of limitations, and the Standard Specification should be consulted.

As discussed in Chapter 2, the material underlying the amorphous peat or muck is often a soft clay or marl. This material can influence the behavior of the constructed embankment. These materials should be sampled as well to determine their effects on embankment behavior. It is advisable to continue sampling until a layer of adequate strength is reached.

EMBANKMENT DESIGN

Embankments constructed over soils of this nature can be designed with or without geotextiles, depending on the initial shear strength of the deposit. In some instances, geotextiles are necessary to allow construction to begin. As discussed in Chapter 2, geotextiles have been found to reduce the horizontal deformations of embankments, increase stability, bridge weak areas of the subsoil, and provide a barrier between embankment and foundation soils. This section will cover the design of embankments with or without geotextiles. Design examples for both procedures are included in Appendix D.

Embankments without Geotextile Reinforcement

After the site investigation, the results of field vane shear tests provide a range of values of the undrained shear strength in the deposit. Rather than using an average value of the shear strength, a conservative value (in some cases the lowest measured value) should be used during design analyses. The variability typical of these soils can result in a considerable amount of variation in shear strength, and the average value could be significantly greater than the measured lower values.

The factor of safety used in this thesis for overall bearing capacity, rotational failure, and lateral squeeze is 1.3. Attewell & Taylor (1984) state that for embankments constructed on a compressible foundation, a factor of safety on the order of 1.5 is ordinarily used during stability analysis. Values as low as 1.2 have been used when soil data and site conditions were well established. When analyzing stability of a preloaded embankment, Stamatopoulos & Kotzias (1985) state that a factor of safety in the range of 1.1 to 1.3 can be used, assuming that the correct input values have been used during analyses. Thus, although a value of 1.3 is used herein, when selecting a factor of safety, considerable judgement based on previous experience should be exercised.

Overall Bearing Capacity: The overall bearing capacity calculation is a simple one. This step is used to find an approximate value of the allowable height. For a strip loading on soils of this nature, the bearing capacity equation reduces to

$$q = cN_c \quad (4.1)$$

where,

q = ultimate pressure (psf)

c = undrained shear strength (psf)

N_c = bearing capacity factor determined from Vesic (1973)

The maximum allowable load providing a factor of safety of 1.3 should be calculated. Once the allowable load is known, the height of this load is found as

$$H = \frac{q_{all}}{\gamma} \quad (4.2)$$

where,

q_{all} = allowable pressure (psf)

γ = unit weight of embankment soil (pcf)

Lateral Squeeze: The weight of an embankment will tend to squeeze the foundation soil laterally. Jurgenson (1937) states that the force required to cause lateral squeeze of a soil between two rigid plates is equal to

$$P = \frac{1}{a} c B L^2 \quad (4.3)$$

where,

P=total applied load (lb)

a=one half of deposit thickness (ft)

c=undrained shear strength (psf)

B=length of embankment (=1 ft for unit length)

L=one half of embankment base width (ft)

A diagram illustrating these variables is provided in Figure 4.1. The total load, P, for the height of the embankment found in the previous step is then calculated for a unit length of embankment. From this, the required value of the undrained shear strength is

$$c_{req} = \frac{Pa}{BL^2} \quad (4.4)$$

The resulting factor of safety ($\frac{c_{avail}}{c_{req}}$) must be greater than

1.3. If this is not the case, the height of the first load may be decreased, or the geometry of the embankment can be adjusted to provide a longer base length¹.

Embankment Spreading: The lateral earth pressure developed within the embankment, as shown in Figure 4.2, must be resisted by shearing stresses at the base. If suf-

1. The authors' attention has been called to a "rule of thumb" which requires that c_{req} be greater than 1/3 of the applied embankment stress. The authors are unable to identify the source of this rule.

ficient resistance is not provided by the foundation, the embankment may become unstable. The lateral earth pressure, P_a , developed within a cohesionless embankment is

$$P_a = 0.5 \gamma H^2 \tan^2 \left(45 - \frac{\phi}{2} \right) \quad (4.5)$$

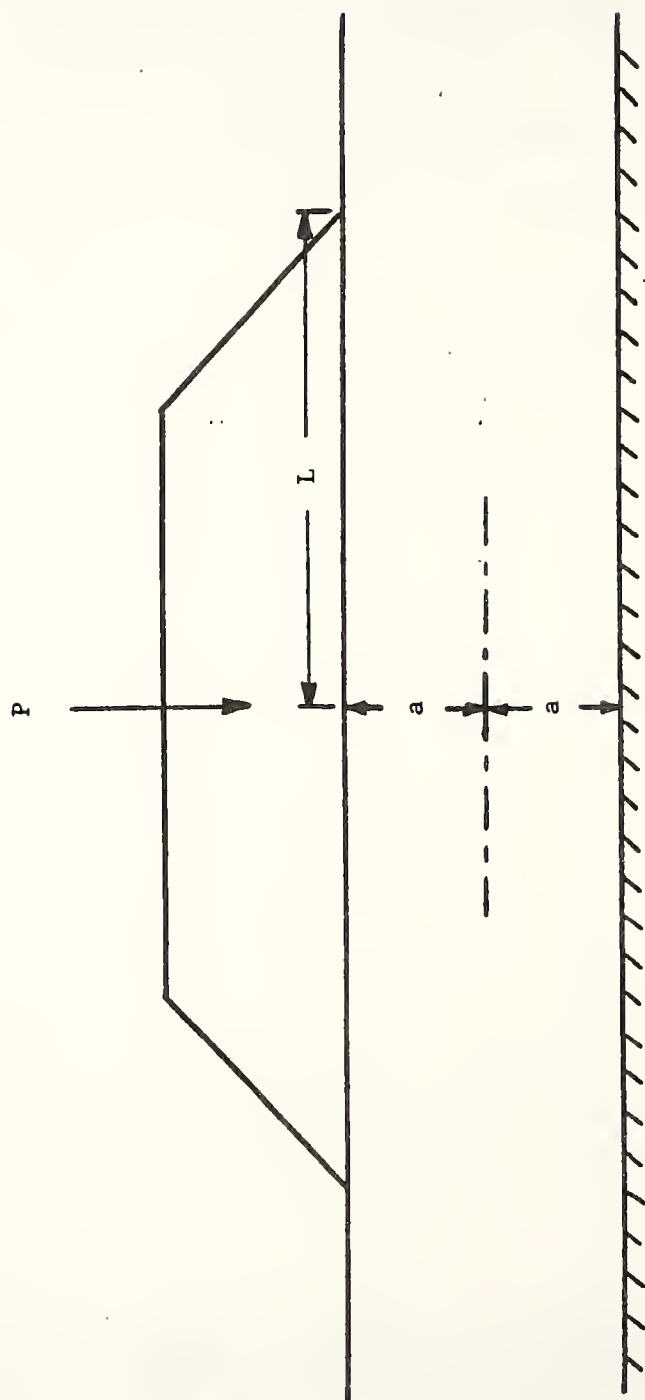


Figure 4.1 Description of Variables in Equation 4.3.

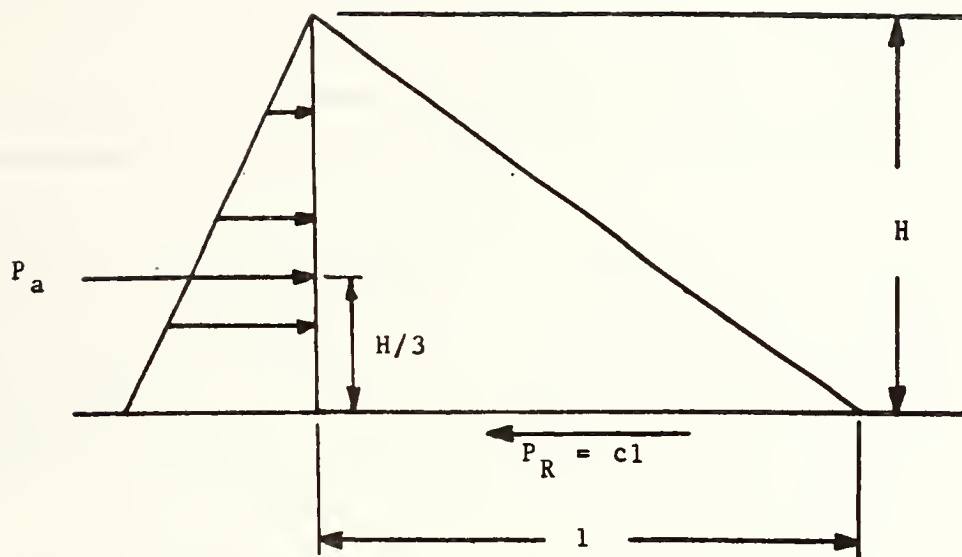


Figure 4.2 Embankment Spreading.

where,

γ =unit weight of embankment soil (pcf)

H =height of embankment (ft)

ϕ =internal angle of friction of embankment soil

The resistance, P_r , provided by the foundation soil is

$$P_r = cl \quad (4.6)$$

where,

c =undrained shear strength (psf)

l =lateral distance from crest to toe of embankment (ft)

A factor of safety of 2 against embankment spreading is suggested for geotextile reinforced embankments (Fowler, 1981) and has been adopted for unreinforced embankments as well. A calculated factor of safety less than this value will require the use of a lesser height of load.

Rotational Failure: To investigate the stability of the embankment with respect to rotational failure, STABL4 (Lovell, Sharma, & Carpenter, 1984) or STABL5 (Carpenter, 1986) should be utilized. The stability analysis should be performed for the allowable embankment height found after the preceding analyses. If the stability analysis yields a factor of safety less than 1.3, another iteration should be performed using a lesser height of load.

Resistance provided by the embankment material in unreinforced embankments may be included in the stability

analysis only if an overconsolidated or dessicated layer exists at the surface of the deposit. Otherwise, any lateral movements in the embankment can create tension cracks, sharply reducing the resistance within the embankment.

Geotextile Reinforced Embankments

If geotextiles are used during embankment construction, the allowable safe height of construction is increased as a result of the stabilizing action of the reinforcement. This section will discuss the design of geotextile reinforced embankments. The information in this section is based on a design manual by Christopher & Holtz (1985). The manual provides a more in-depth coverage of the topic, and is recommended reading when designing with geotextiles.

Overall Bearing Capacity: The overall bearing capacity is calculated in the same manner as for the unreinforced embankments. Once again, the recommended factor of safety is 1.3. Once the allowable pressure is calculated, the safe height can be calculated. For geotextile reinforced embankments, the average applied pressure can be estimated as $\frac{P}{2L}$, where P and L are as illustrated in Figure 4.1.

Lateral Squeeze: Geotextiles have no influence on the extent of lateral squeeze. The required value of the undrained shear strength is therefore found in the same

manner as unreinforced embankments. Embankments constructed with geotextiles require a factor of safety of 1.3 against lateral squeeze.

Rotational Failure: Using STABL6 (Humphrey, 1986), a stability analysis should be performed for the calculated height of load. The value of the fabric strength required should be adjusted until the minimum factor of safety is 1.3.

Embankment Spreading: When constructing embankments with geotextiles, the lateral earth pressures exerted by the fill are resisted by the reinforcement. If sufficient friction is not developed between the embankment and the reinforcement, or the foundation and the reinforcement, the embankment may become unstable. Instability may also occur if the foundation soils beneath the embankment can not resist the applied shear stress.

These two failure modes dictate that the reinforcement must provide enough frictional resistance to prevent sliding along the interface. In addition, the tensile strength of the geotextile must be adequate to prevent rupture or tearing. The lateral earth pressure developed within a cohesionless embankment is given in Equation 4.5. The resisting force, P_r , provided by the geotextile is found as

$$P_r = 0.5 \gamma l H \tan \phi_{sf} \quad (4.7)$$

where,

ϕ_{sf} = soil fabric friction angle

l = lateral distance from crest to toe of embankment (ft)

The value of ϕ_{sf} is equal to

$$\phi_{sf} = \tan^{-1}(4P_a / \gamma l H) \quad (4.8)$$

The specified value of ϕ_{sf} should be at least $\frac{2}{3} (\phi_{soil})$.

A factor of safety against embankment spreading is found by dividing the resisting force by the actuating forces. A minimum factor of safety of 2 is recommended by Fowler (1981).

The lateral earth pressures must be resisted by tension forces in the reinforcement. To prevent splitting or tearing, Fowler recommends a minimum factor of safety of 1.5. The resulting required fabric strength is

$$T_f = 1.5 P_a \quad (4.9)$$

where T_f equals fabric tension.

Limit Fabric Deformation: The stresses required to resist lateral spreading are developed through strain in the geotextile. The modulus of the geotextile controls the amount of strain. The resulting distribution from lateral spreading is assumed to vary linearly from zero at the toe to its maximum value beneath the crest of the embankment.

This assumption is unconservative in view of the fact that a majority of geotextiles possess stress-strain curves that develop concave-upward, not linearly. A factor of safety equal to 1.5 should be used to determine the geotextile tensile modulus, E_f . If the required modulus is calculated from the tensile strength, T_f , the factor of safety is included. The minimum geotextile tensile modulus, E_f , required is found as

$$E_f = \frac{T_f}{\epsilon_{\max}} \quad (4.10)$$

where ϵ_{\max} is the maximum strain in percent expected in the geotextile along the embankment centerline.

Using the assumed linear strain distribution, the maximum strain is two times the average strain beneath the embankment. A value of 5% average strain is recommended for design. The maximum strain would then be 10%, and the required fabric tensile modulus may be found as

$$E_f = 10T_f \quad (4.11)$$

The embankment will also deform until the required fabric strain develops to prevent a rotational stability failure. The actual behavior of the embankment in this condition is unknown, and assumptions outlined in Christopher & Holtz (1985) have been used. The resulting minimum required modulus to control a rotational failure is found as

$$E_{fr} = \frac{T_{fr}}{0.10} \quad (4.12)$$

where,

T_{fr} = required tensile strength of fabric

E_{fr} = minimum fabric modulus

STAGE LOADING

As mentioned previously, the soft nature of amorphous peats and mucks often makes construction to the full height in one stage impossible, particularly if a surcharge is to be placed. Construction will therefore have to be performed in stages. Once the maximum first load, as calculated in the preceding analyses, has been applied, the foundation will begin to consolidate. The consolidation will result in a strength gain allowing further loads to be placed without inducing failure in the embankment foundation.

To determine the duration of each stage load required for consolidation to occur, pore pressure transducers as shown in Figure 4.3 should be placed in the foundation. Once excess pore pressures induced by the previous loading have dissipated, no further strength gain will develop. Field vane shear tests should then be performed in the foundation beneath the embankment, and in areas adjacent to the embankment to determine the extent of the strength gain. Using the increased values of undrained shear strength, the aforementioned analyses should be performed to calculate the allowable height of the second stage load. This procedure

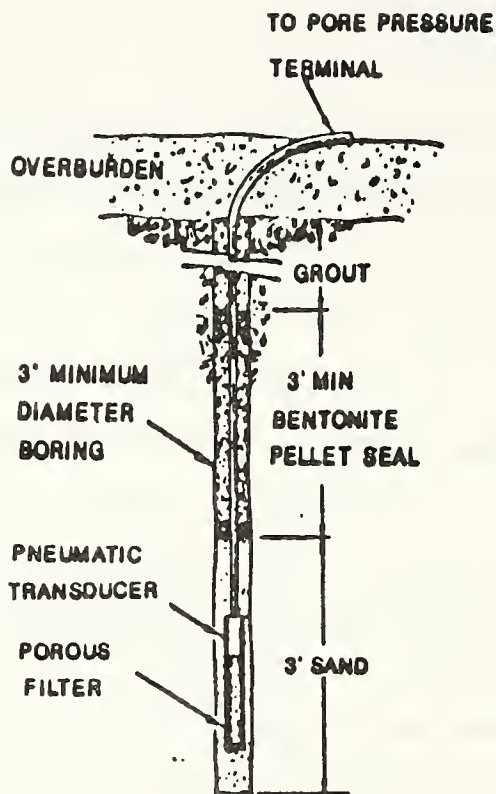


Figure 4.3 Pore Pressure Transducer Installation.
From Slope Indicator Company.

of applying the load, allowing pore pressures to dissipate, measuring the increased shear strength, and placing subsequent loads should continue until the final embankment height is reached.

PRELOADING

One of the problems associated with the construction of highway embankments over amorphous peat and muck is the large amount of secondary compression taking place over an extended period of time. To reduce the amount of settlement that occurs during the service life of an embankment, a surcharge in excess of the final design embankment height should be placed. The necessary height of surcharge is found by first using the Gibson-Lo model to predict settlements induced by the design height of the embankment. As discussed in Chapter 2, the input parameters required for this model are obtained from the results of creep tests. In order to obtain the most accurate results, the creep tests should not be performed at conventional load increment ratios. Instead, they should be performed at stress levels simulating actual field loading.

Creep testing begins by reconsolidating the samples at their preconsolidation pressure in the loading frame. Edil & Simon-Gilles (1986) recommend sustaining the load until deformation is reduced to 0.001 to 0.003 mm/day. At this

point, the next load is applied corresponding to the stress level induced by the design embankment height. The load should be sustained until enough data are collected to accurately calculate the values required for the Gibson-Lo model. For the materials tested during this project, a load duration of 10,000 minutes was found to be sufficient.

Once creep tests are completed, a plot of log strain rate versus time, such as in Figure 4.4, should be constructed. Then, using the method presented by Lo, Bozozuk, and Law (1976), the values of a_{lab} , b_{lab} , and $(\frac{\lambda}{b})_{lab}$ are found by using the values obtained from the Figure and solving Equations 2.2 through 2.4 simultaneously.

As discussed in Chapter 2, the values of a_{lab} and a_{field} are approximately equal for similar stress levels. The values of b_{lab} and $(\frac{\lambda}{b})_{lab}$ must be corrected to corresponding field conditions. Figure 2.3 is used to find the value of b_{field} . The value of $(\frac{\lambda}{b})_{field}$ can be determined from Figure 2.4. If the field strain rate is not known from previous experience, Edil & Mochtar (1984) recommend using a value two to three orders of magnitude smaller than that observed in the laboratory.

It should be recognized that the recommended correlations in Figures 2.1 through 2.4 are best fit lines through data with a considerable amount of scatter, and thus these

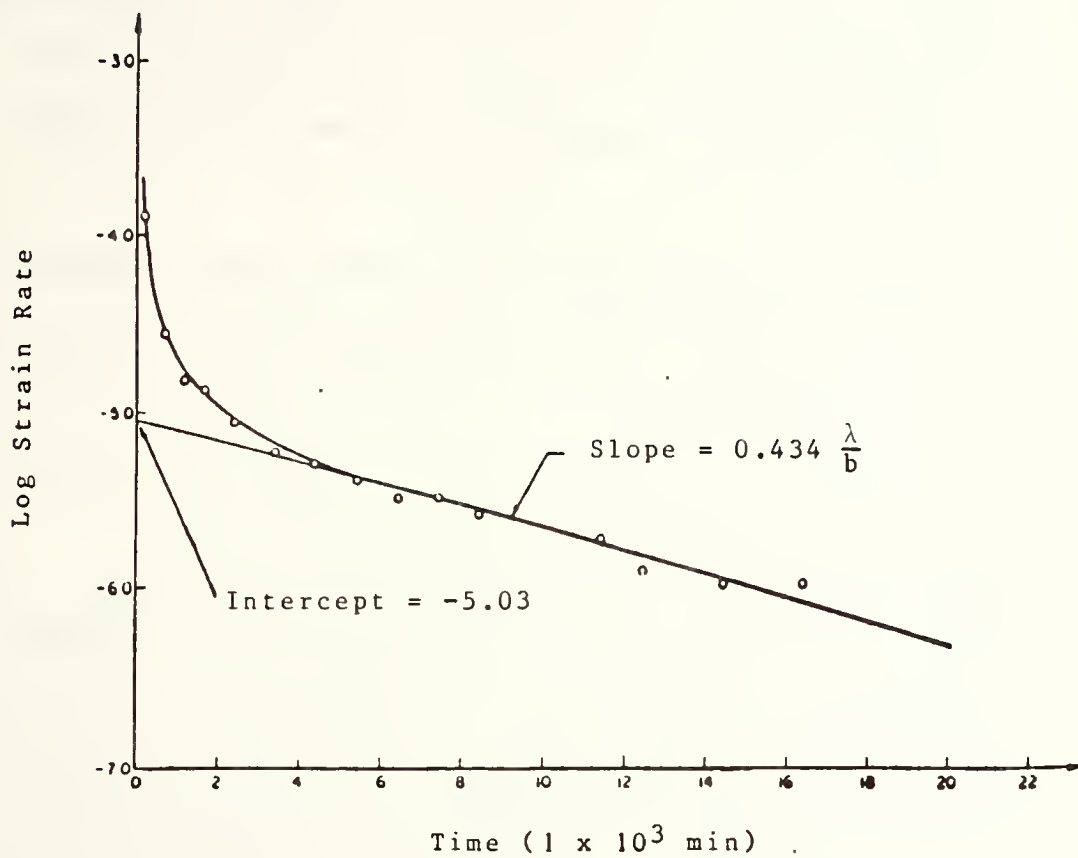


Figure 4.4 Plot of Log Strain Rate with Time from Laboratory Tests. From Lo, Bozozuk, and Law (1976).

correlations provide only an approximate relationship between laboratory and field performances. Their use can help improve predictions, however they still may not provide sufficient reliability, and they should be used with caution. As a result, the use of laboratory test results for settlement prediction is still questionable. The most reliable settlement predictions can be obtained by observing field performance for calculation of the Gibson-Lo model parameters.

Using the corrected parameters, settlement prediction can now be conducted using the Gibson-Lo model. To facilitate these calculations, two computer programs are provided in Appendix C. The first program, GIBSON.F, calculates the parameters of the Gibson-Lo model, and the second, PREDICT.F, provides a prediction of the strain within the deposit. The resulting settlement values are calculated by multiplying the strain values by the thickness of the deposit being analyzed. Both programs are written in FORTRAN for use on the IBM PC. The use of these programs for a specific case will be illustrated in the design examples of Appendix D.

From the results of the settlement prediction, the amount of settlement expected within the service life of the embankment can be found. The objective of the surcharge is to induce that amount of settlement during the time required

for primary consolidation. To calculate the height of surcharge required to accomplish this, the Gibson-Lo model should be used to predict the settlement induced by various heights of surcharge until the appropriate value is obtained. The results of creep tests simulating loading by the design embankment height may be used as long as the stress increase of the surcharge plus the embankment is less than twice that used during these tests, as concluded by Gruen (1983). Once the height of surcharge is determined, the preceding analyses presented regarding embankment design must be performed to ensure that the surcharge does not create any instabilities.

FIELD OBSERVATIONS

To aid in monitoring the behavior of the deposit of amorphous peat or muck when loaded, a number of field observations should be made. The most obvious of these is a record of settlements along the embankment centerline. These measurements can be compared with the predicted settlements to check their accuracy. They can also be used to calculate the field strain rate of the deposit, to allow for correction of the rate factor for settlement prediction if required. Settlement measurements will also be used to determine when the required amount of settlement has occurred, allowing for removal of the surcharge.

Inclinometers should also be placed in the embankment site to measure any lateral movements of the embankment. A typical inclinometer, designed by the Swedish Geotechnical Institute, is illustrated in Figure 4.5. Data obtained from inclinometers should be interpreted carefully, as these soft materials can flow around the inclinometer. As mentioned previously, pore pressure transducers should be installed to observe the dissipation of excess pore pressures. All types of field instrumentation should be installed to provide redundancy. This will allow for any equipment that becomes inoperable or is disturbed during construction.

EMBANKMENT MATERIALS

Deposits of amorphous peat or muck are in low-lying areas and are very wet. Therefore, portions of the embankment will become saturated, particularly as settlement occurs. As a result of this, a well graded material possessing a limited amount of fines should be chosen for construction above the water table. This will allow for embankment drainage and will reduce the effects of wetting/drying or freezing/thawing.

CONSTRUCTION SEQUENCE

Barsvary et. al. (1984) present a sequence of construction for embankments over soft subsoils. A diagram of their procedure is illustrated in Figure 4.6. Before actual

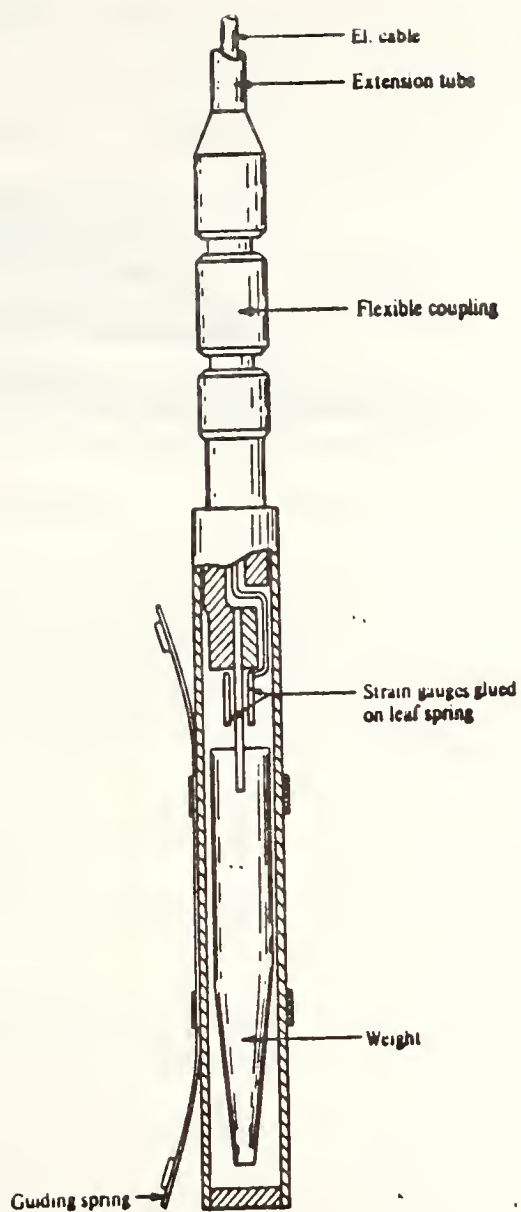
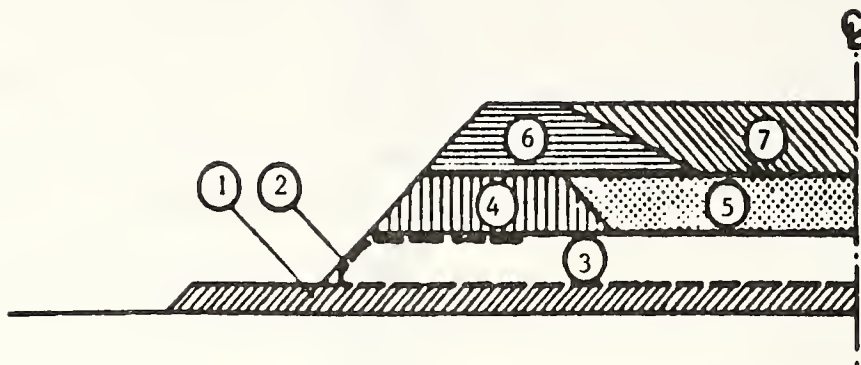


Figure 4.5 Inclinator Type SGI. From Winterkorn & Fang (1975).



STAGE I

1. Place working platform
2. Place geotextile transverse to alignment
3. Place 0.3 m granular and fold back geotextile
4. Place and compact earth to anchor geotextile
5. Place and compact embankment core

STAGE II

6. Place and compact earth to profile grade at edges
7. Place and compact earth to profile grade at core

Figure 4.6 Construction Sequence. From Barsvary et al. (1982).

construction begins, they recommend placing a working platform on the foundation soil for construction mobility and easier placement of the geotextile. If geotextiles are to be used, they should be placed on the working platform, transverse to the alignment of the embankment. After placing the embankment to a height of one foot, the geotextile should be folded back on top of this material as shown in the Figure. The geotextile should then be anchored by compacting earth above the folded region as in Step 4. The core of the embankment is then placed and compacted. Subsequent lifts should then be constructed by placing and compacting the edges as shown in Step 6, followed by placement and compaction of the embankment core. Compaction lifts should be kept at about the same level, to aid compaction by lateral constraint.

CHAPTER V-CONCLUSIONS AND RECOMMENDATIONS

CONCLUSIONS

This report has investigated the problems associated with the construction of low (± 10 ft) highway embankments over amorphous peats and mucks. A number of conclusions have been drawn as a result of this research:

1. Based on previous work by Gruen (1983) and Joseph (1986), it is felt that the Gibson-Lo model is the best method of predicting the long-term compression of organic soils.
2. The use of relationships developed by Edil & Mochtar (1984) correlating the results of laboratory tests with field behavior will improve the results of settlement predictions made with the Gibson-Lo model. However, these correlations are approximations and they should be used with caution.
3. The use of K_0 triaxial testing for the determination of the undrained shear strength of a foundation beneath an embankment loading is unfeasible, both technically and economically.

4. Field vane shear testing is a more practical method of measuring the undrained shear strength. This method allows for more rapid determination of shear strength, and eliminates the need for assumptions regarding the extent of consolidation beneath and adjacent to the embankment by making direct measurements. The limitations of vane shear testing, as discussed in Chapter 3, should be considered when interpreting test results.

5. In order to construct embankments over deposits of amorphous peat or muck, stage loading will be required in most instances, especially when a surcharge is to be applied. The strength gain from consolidation will allow the placement of subsequent loads without inducing failure in the foundation.

6. To reduce the amount of settlement experienced during the service life of the embankment, a surcharge should be placed to accelerate compression of the foundation.

7. A procedure for the design and construction of low embankments (± 10 ft) over amorphous peats and mucks has been developed, and is presented in Chapter 4.

RECOMMENDATIONS

Based on the findings of this report, a number of recommendations have been made:

1. The construction procedure outlined in this report should be utilized for construction of low embankments (± 10 ft) over amorphous peat and muck.
2. For deposits of these materials that are extremely soft, geotextiles may be required for successful construction. To supplement the information provided in this report, the reference by Christopher & Holtz (1985) should be consulted.
3. A test embankment should be constructed over a deposit of amorphous peat or muck, including installation of pressure transducers, inclinometers, and settlement plates. The test embankment should be used to prove the usefulness of the recommended procedure for design and construction.
4. As this procedure is implemented, the results of field performance should be collected for development of figures correlating laboratory and field behaviors similar to Figures 2.1 through 2.4.

LIST OF REFERENCES

LIST OF REFERENCES

1. ASTM Standard Specification D854-83, "Standard Test Method for Specific Gravity of Soils," 1986 Annual Book of ASTM Standards, Vol. 04.08.
2. ASTM Standard Specification D2573-72, "Standard Test Method for Field Vane Shear Test in Cohesive Soil", 1986 Annual Book of ASTM Standards, Vol. 04.08.
3. ASTM Standard Specification D2974-84, "Standard Test Methods for Moisture, Ash, and Organic Matter of Peat Materials," 1986 Annual Book of ASTM Standards, Vol. 04.08.
4. ASTM Standard Specification D4318-84, "Standard Test Methods for Liquid Limit, Plastic Limit, and Plasticity Index of Soils," 1986 Annual Book of ASTM Standards, Vol. 04.08.
5. ASTM Standard Specification D 4544-86, "Standard Practice for Estimating Peat Deposit Thickness," 1986 Annual Book of ASTM Standards, Vol. 04.08.
6. Attewell, P.B. and Taylor, R.K. (1984) "Ground Movements and their Effects on Structures," Surrey University Press, London, 441 pp.
7. Barsvary, A.K., MacLean, M.D. and Cragg, C.B.H. (1982) "Instrumented Case Histories of Fabric Reinforced Embankments over Peat Deposits," Proceedings Second International Conference on Geotextiles, Las Vegas, Vol. 3, pp. 647-652.
8. Bjerrum, Laurits (1972) "Embankments on Soft Ground," Proceedings of ASCE Specialty Conference on Performance of Earth and Earth Supported Structures, Purdue University, Vol. 2, pp. 1-54.
9. Bjerrum, L., Clausen, C.J.F. and Duncan, J.M. (1972) "Earth Pressures on Flexible Structures: A State of the Art Report," Proceedings Fifth European Conference on Soil Mechanics and Foundation Engineering, Madrid, Vol. 2, pp. 169-196.

10. Boutrup, E. and Holtz, R.D. (1983) "Fabric Reinforced Embankments Constructed on Weak Foundations," Final Report, Joint Highway Research Project, Project No. C-36-3 M, File 6-14-13.
11. Campanela, R.G. and Vaid, Y.P. (1972) " A Simple K₀ Triaxial Cell," Canadian Geotechnical Journal, Vol. 9, pp. 249-260.
12. Carpenter, James R. (1986) "STABL5/PC STABL5 USER MANUAL," JHRP-86/14, Joint Highway Research Project, Purdue University, West Lafayette, Indiana.
13. Christopher, B.R. and Holtz, R.D. (1985) "Geotextile Engineering Manual," Prepared for Federal Highway Administration, National Highway Institute, Washington, D.C.
14. Dhowian, A.W. and Edil, T.B. (1980) "Consolidation Behavior of Peats," Geotechnical Testing Journal, American Society for Testing and Materials, Vol. 3, No. 3, pp. 105-114.
15. Edil, Tuncer B. and Mochtar, Noor E. (1984) "Prediction of Peat Settlement," Proceedings, Sedimentation/Consolidation Models, American Society of Civil Engineers, San Francisco California, pp. 411-424.
16. Edil, Tuncer B. and Simon-Gilles, Dixie A. (1986) "Settlement of Embankments on Peat: Two Case Histories," Advances in Peatlands Engineering, National Research Council Canada, Ottawa, Canada, pp. 1-8.
17. Fowler, J. (1981) "Design, Construction, and Analysis of Fabric-Reinforced Embankment Test Section at Pinto-Pass, Mobile, Alabama," Technical Report EL-81-8, USAE Waterways Experiment Station, Vicksburg, Mississippi, 238 pp.
18. Gruen, H.A. Jr. (1983) "Use of Peats as Embankment Foundations," MSCE Thesis, School of Civil Engineering, Purdue University, West Lafayette, Indiana, 149 pp.
19. Gruen, H.A. Jr. and Lovell, C.W. (1983) "Controlling Movements of Embankments Over Peats and Marls," IN/JHRP-83/6, Joint Highway Research Project, Purdue University, West Lafayette, Indiana, 180 pp.
20. Hannon, J. (1982) "Fabrics Support Embankment Construction over Bay Mud," Proceedings Second International Conference on Geotextiles, Las Vegas, Vol. 3, pp. 653-658.

21. Hollingshead, Garry W. and Raymond, Gerald P. (1971) "Prediction of Undrained Movements Caused by Embankments on Muskeg," Canadian Geotechnical Journal, Vol. 8, pp. 23-35.
22. Humphrey, D.N. (1986) "Design of Reinforced Embankments," Ph.D. Thesis, School of Civil Engineering, Purdue University, West Lafayette, Indiana, December 1986.
23. Hutchins, R.D. (1982) "Behaviour of Geotextiles in Embankment Reinforcement," Proceedings Second International Conference on Geotextiles, Las Vegas, Vol. 3, pp. 617-619.
24. Joseph, P.G. (1986) "Behavior of Mucks and Amorphous Peats as Embankment Foundations," MSCE Thesis, School of Civil Engineering, Purdue University, West Lafayette, IN.
25. Jurgenson, Leo (1934) "The Shearing Resistance of Soils," Contributions to Soil Mechanics 1925-1940, Boston Society of Civil Engineers, pp. 184-217.
26. Krizek, Raymond J. and Sheeran, Donald E. (1970) "Slurry Preparation and Characteristics of Samples Consolidated in the Slurry Consolidometer," Northwestern University, for U.S. Army Corps of Engineers Waterways Experiment Station, Vicksburg, Mississippi.
27. Lambe, T.W. and Whitman, R.V. (1979) "Soil Mechanics," John Wiley & Sons, New York, 553 pp.
28. Landva, A. (1986) "In-Situ Testing of Peat," Use of In Situ Tests in Geotechnical Engineering, Proceedings of In Situ '86, Geotechnical Special Pub. No. 6, pp. 191-220.
29. Lefebvre, G. et al. (1984) "Laboratory Testing and In Situ Behavior of Peat as Embankment Foundations," Canadian Geotechnical Journal, Vol. 21, No. 2, pp. 322-337.
30. Lo, K.Y., Bozozuk, M., and Law, K.T. (1976) "Settlement Analysis of the Gloucester Test Fill," Canadian Geotechnical Journal, Vol. 13, No. 4, pp.339-354.
31. Lovell, C.W., Sharma, S.S. and Carpenter, J.R. (1984) "Slope Stability Analysis with STABL4," JHRP-84/19, Joint Highway Research Project, Purdue University, W. Lafayette, Indiana.

32. MacFarlane, I.C. (1969), Muskeg Engineering Handbook, Muskeg Subcommittee of NRC Associate Committee on Geotechnical Research, University of Toronto Press, 1969.
33. Mitchell, W.K. and Villet, W.C.B. (1987) "Reinforcement of Earth Slopes and Embankments," National Cooperative Highway Research Program Report 290, Transportation Research Board, Washington, D.C., June, 323 pp.
34. Petrik, P.M., Baslik, R. and Leitner, F. (1982) "The Behavior of Reinforced Embankment," Proceedings Second International Conference on Geotextiles, Las Vegas, Vol. 3, pp. 631-634.
35. Raymond, Gerald P., (1969) "Construction Method and Stability of Embankments on Muskeg," Canadian Geotechnical Journal, Vol. 6, No. 1, pp. 81-96.
36. Slope Indicator Company "Geotechnical, Geophysical, Groundwater and Structural Instrumentation," Seattle, Washington.
37. Stamatopoulos, A.C. and Kotzias, P.C. (1985) "Soil Improvement by Preloading," John Wiley & Sons, New York, 256 pp.
38. Tavenas, F. and Leroueil, S. (1977) "Effects of Stresses and Time on the Yielding of Clays," Proceedings, Ninth International Conference on Soil Mechanics and Foundation Engineering, Tokyo, Vol. 1, pp. 319-326.
39. Terzaghi, K. and Peck, R.B. (1967) "Soil Mechanics in Engineering Practice," Second Edition, John Wiley & Sons, Inc., New York.
40. Vesic, A.A. (1973) "Analysis of Ultimate Loads of Shallow Foundations," Journal of the Soil Mechanics and Foundation Division, Vol. 99, No. SM1, pp. 45-73.
41. Watson, G.H., Crooks, J.H.A., Williams, R.S. and Yam, C.C. (1984) "Performance of Preloaded and Stage-Loaded Structures on Soft Soils in Trinidad," Geotechnique, Vol. 34, No. 2, pp. 239-257.
42. Weber, W.G., Jr. (1969) "Performance of Embankments Constructed over Peat," ASCE Proceedings, Vol. 95, No. SM1, pp. 53-76.
43. Winterkorn, H.F. and Fang, H-Y (1975) "Foundation Engineering Handbook," Van Nostrand Reinhold Company,

APPENDICES

APPENDIX A: CREEP TEST RESULTS

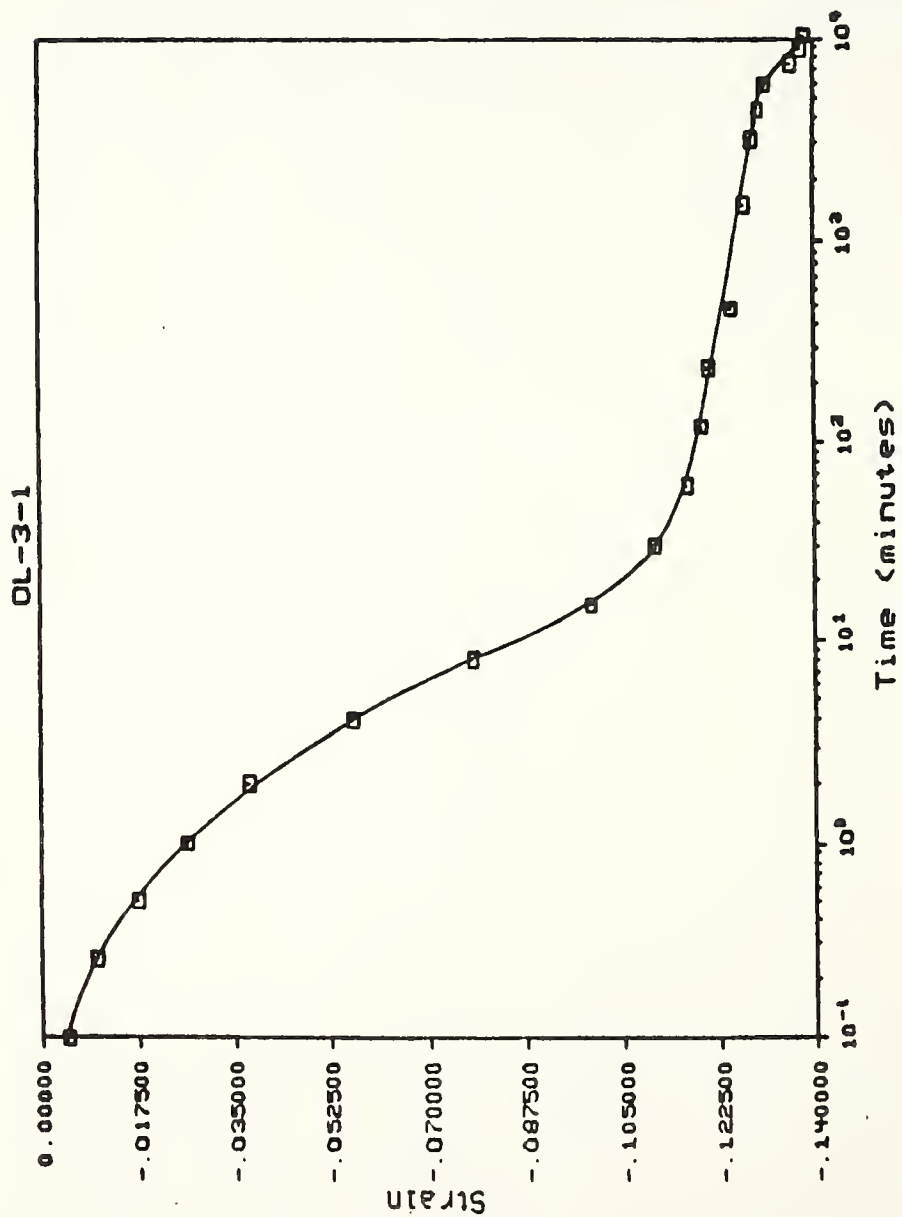


Figure A1 Strain versus Logarithm Time, Creep Test OL-3-1.

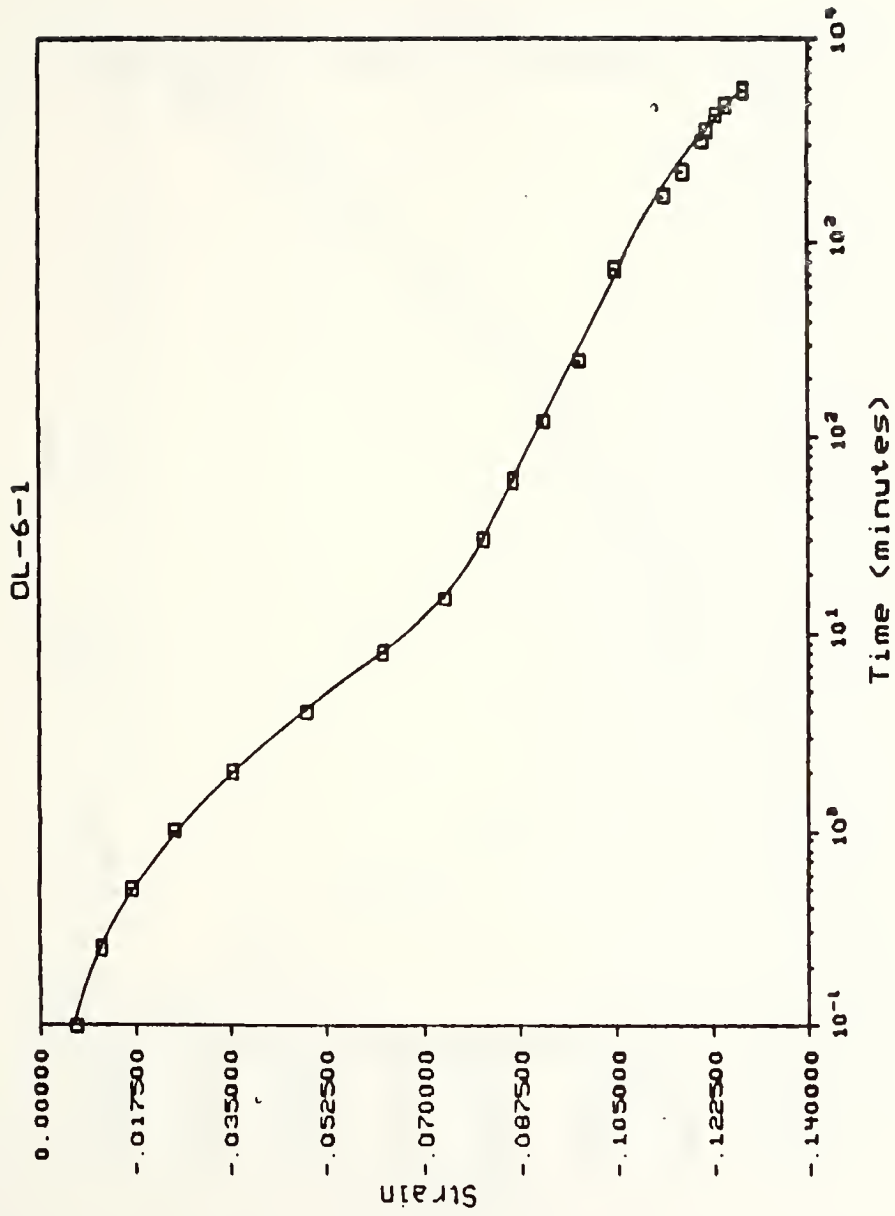


Figure A2 Strain versus Logarithm Time, Creep Test OL-6-1.

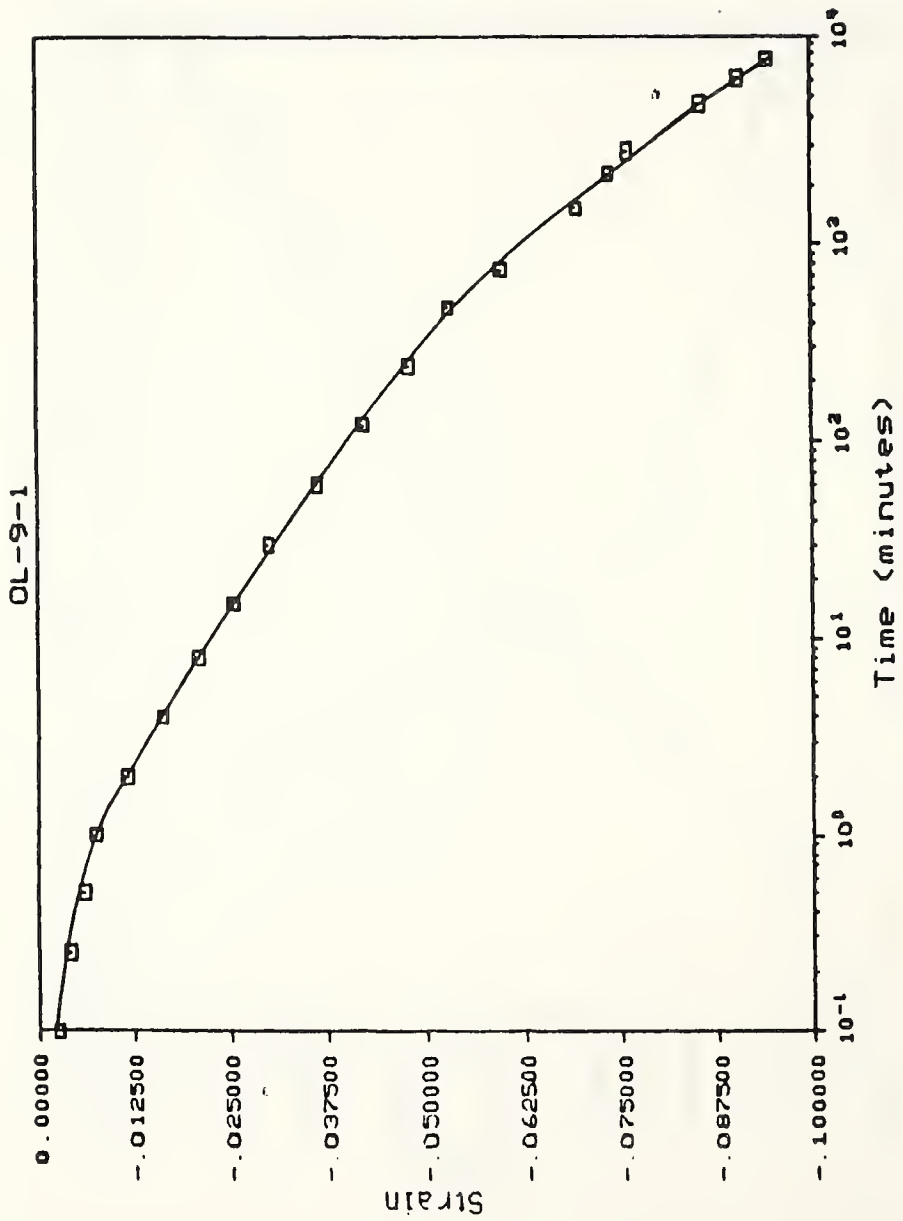


Figure A3 Strain versus Logarithm Time, Creep Test OL-9-1.

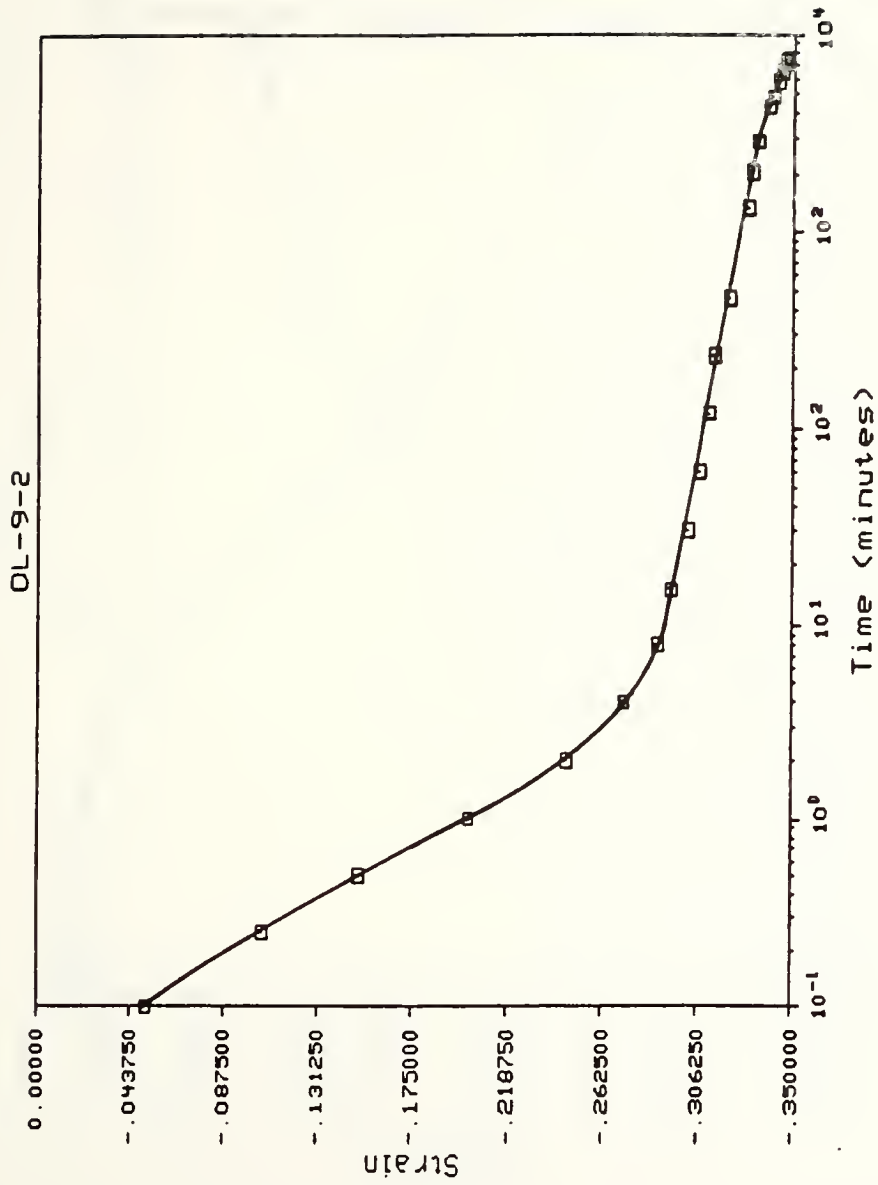


Figure A4 Strain versus Logarithm Time, Creep Test OL-9-2.

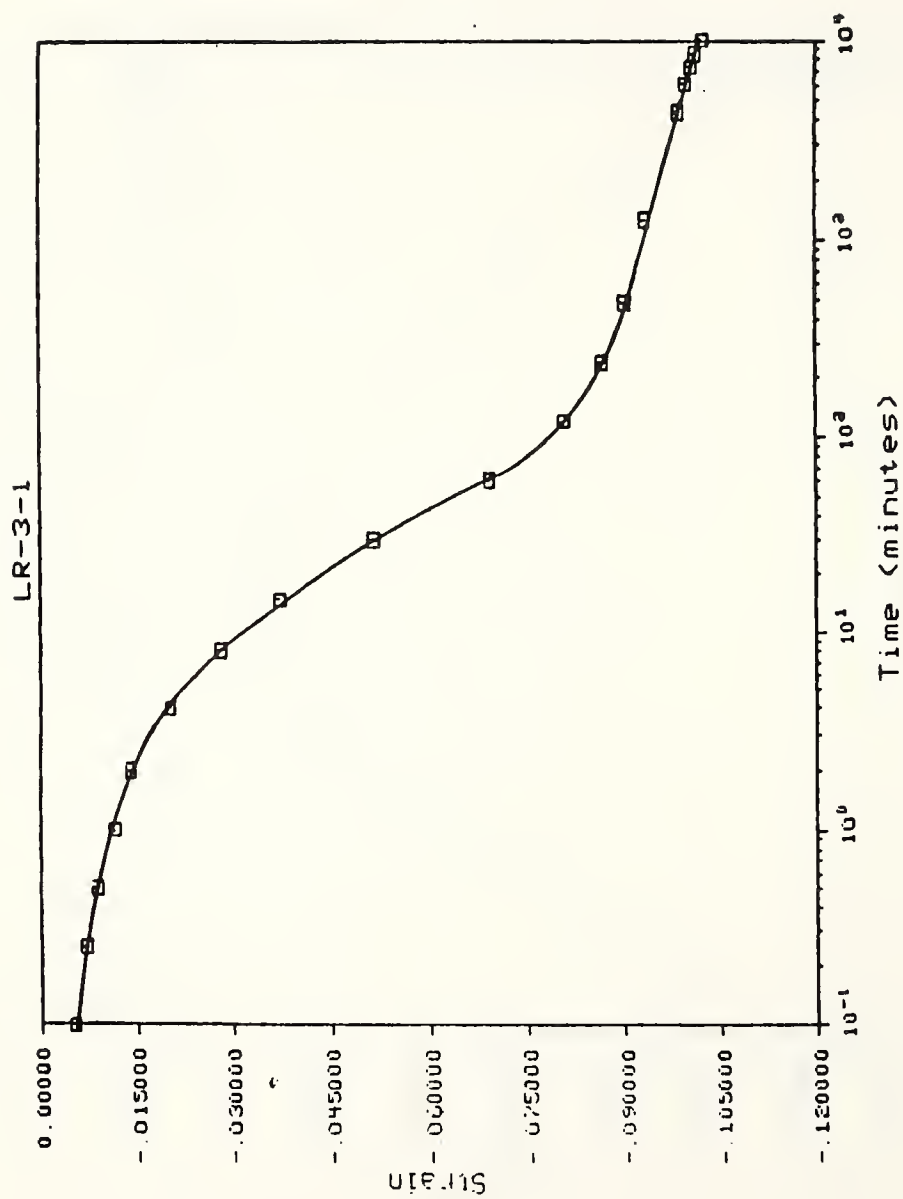


Figure A5 Strain versus Logarithm Time, Creep Test LR-3-1.

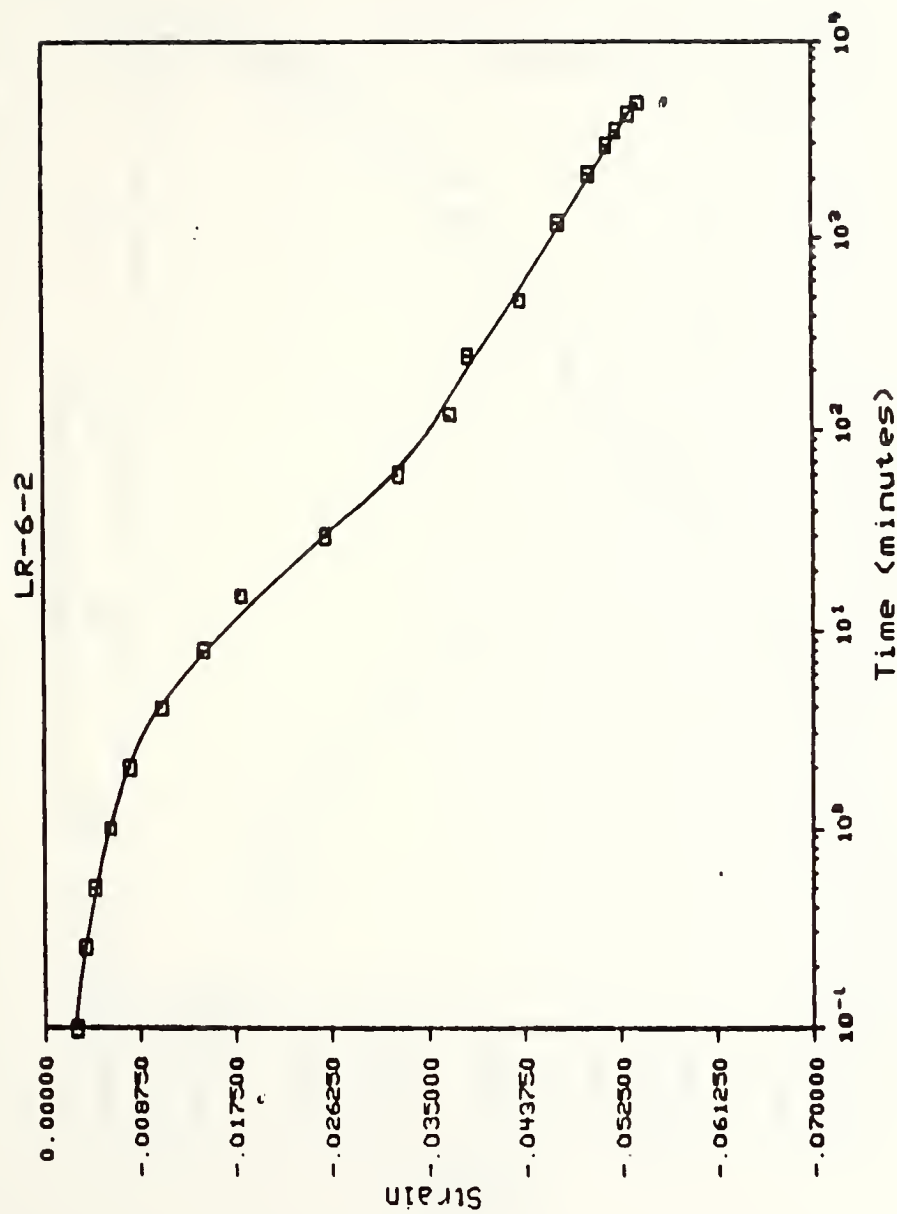


Figure A6 Strain versus Logarithm Time, Creep Test LR-6-2.

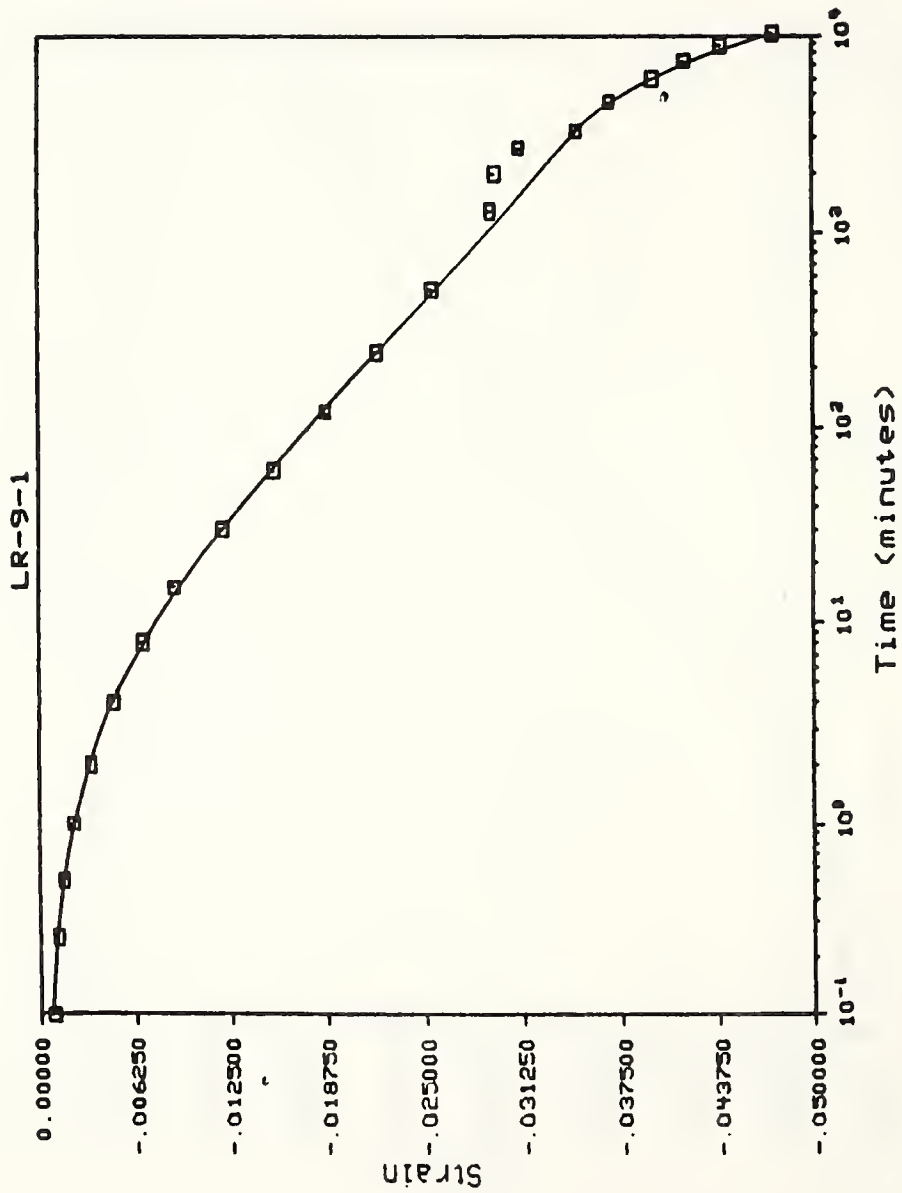


Figure A7 Strain versus Logarithm Time, Creep Test LR-9-1.

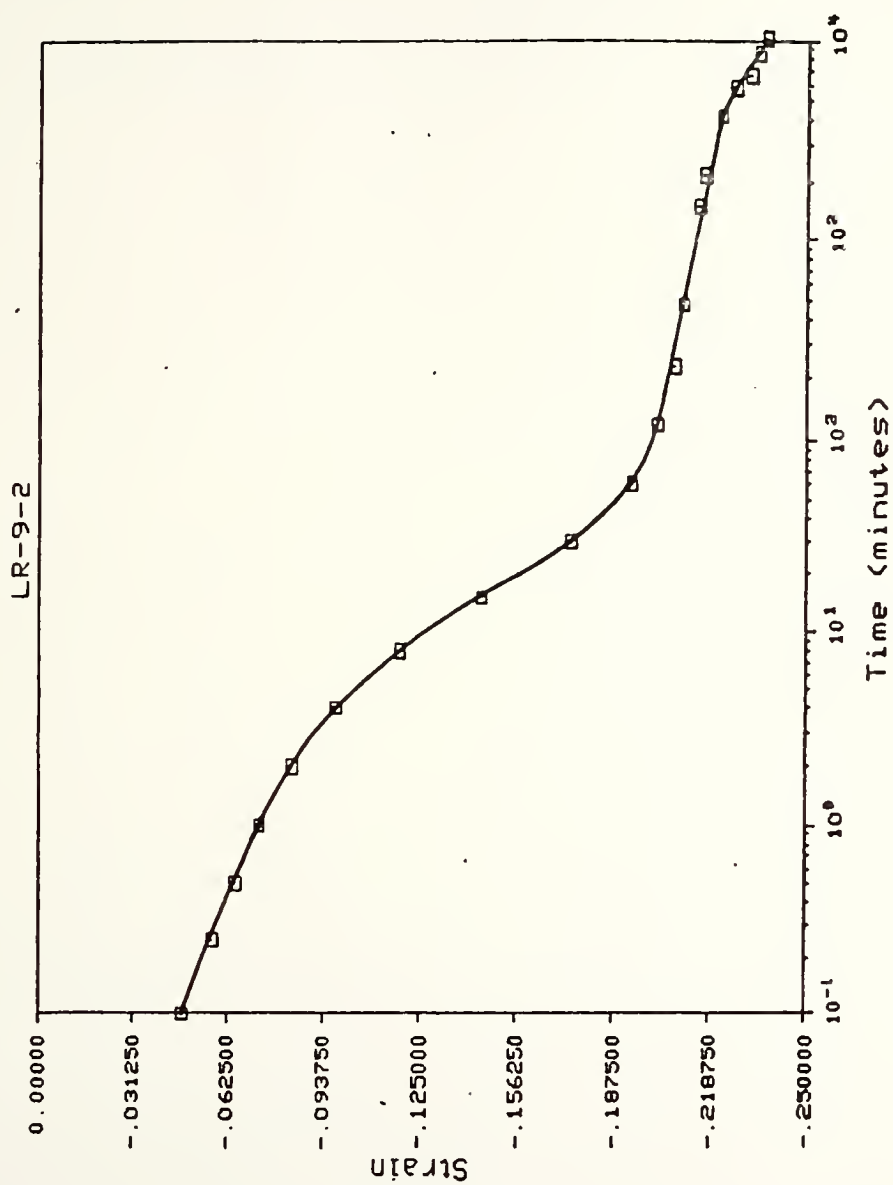


Figure A8 Strain versus Logarithm Time,
Creep Test LR-9-2.

APPENDIX B: K_0 TRIAXIAL TEST CHECK LIST

Date _____

Test No. _____

K₀ Triaxial Test Check List

Specimen Installation

- 1) Place sample on the bottom pedestal with the plastic former on ()
- 2) Fasten O rings on bottom pedestal..... ()
- 3) Install top platen ()
- 4) Remove the plastic former ()
- 5) Connect the drainage lines to top platen..... ()
- 6) Check position of sample ()
- 7) Place cell wall ()
- 8) Place top lid with piston locked at position leaving room for six inch sample ()
- 9) Tighten the top rod nut ()
- 10) Place rods and fasten top lid securely ()
- 11) Place piston top and strain gage ()
- 12) Place the load cell, check level and position of triaxial cell ()
- 13) Lock the load cell frame ()
- 14) Attach counterweights ()

Date _____

Test No. _____

 K_0 Triaxial Test Check List

Specimen Saturation

- 1) Open the cell top drainage valve ()
- 2) Place transducers, connect drainage lines..... ()
- 3) Pump water into the cell ()
- 4) Drain the cell transducer port ()
- 5) Close the top cell valve ()
- 6) Shut all valves at cell bottom ()
- 7) Apply cell pressure of 6 psi, pore
 pressure of 5 psi ()
- 8) Open cell valve ()
- 9) Open drainage valves ()
- 10) Flush top and bottom platens ()
- 11) Flush cell top valve ()
- 12) Lock Bellofram piston ()
- 13) Unlock piston ()
- 14) Switch drainage lines to PWP ()
- 15) Record burette, DCDT, and load cell readings ()
- 16) Increase cell, pore, and Bellofram pressure ()

Date _____

Test No. _____

K₀ Triaxial Test Check List

Preliminary Consolidation

- 1) Record DCDT, pore and cell pressures ()
- 2) Lock drainage lines ()
- 3) Increase cell and Bellofram pressures ()
- 4) Wait for pore pressure to stabilize ()
- 5) Record initial readings ()
- 6) Lock the cell ()
- 7) Open drainage lines and start timer ()

Axial Loading

- 1) Lock Bellofram piston ()
- 2) Adjust cell pressure ()
- 3) Open cell line ()
- 4) Lock drainage lines ()
- 5) Adjust axial pressure and hand crank
the load frame ()
- 6) Wait for pore pressure to stabilize ()
- 7) Check time ()
- 8) Start the motor ()

APPENDIX C: COMPUTER PROGRAMS

```
C ****  
C *****  
C ***** GIBSON.F *****  
C *****  
C ****  
C  
C This program was developed to calculate the parameters required  
C for the Gibson-Lo model using the method developed by Lo,  
C Bozozuk, and Law (1976).  
C  
C *****  
C *****  
C DEFINITION OF VARIABLES  
C  
C e = coefficient of primary compression from Lo, Bozozuk and  
C     Law  
C lambda = lambda from method of Lo, Bozozuk and Law  
C b = coefficient of secondary compression from Lo, Bozozuk  
C deltasig = stress increase for creep test  
C esubf = last strain reading in secondary compression  
C ratef = rate factor from method of Lo, Bozozuk and Law  
C         equals lambda/b  
C slope = line slope from method of Lo, Bozozuk and Law  
C trcpt = y-intercept from method of Lo, Bozozuk and Law  
C tsubf = time of last strain reading corresponding to esubf  
C *****  
C *****  
C *****  
C Read in y-intercept, line slope, last strain reading, time of  
C last strain reading, and stress increase  
C *****  
C write(6,100)  
100 format(/2x,'Enter y-intercept, slope, last strain reading',  
?/2x,'time of last strain reading, and stress increase:')  
read(6,*) trcpt, slope, esubf, tsubf, deltasig  
C *****  
C Calculate parameters for Gibson-Lo model using method developed  
C by Lo, Bozozuk and Law  
C *****  
ratef=slope/0.434  
lambda=(10.0**trcpt)/deltasig  
b=lambda/ratef  
a=(esubf/deltasig)-b*(b**exp(-ratef*tsubf))  
write(6,*)'GIBSON.F OUTPUT'  
write(6,*)  
write(6,*)'The calculated value of a equals',a  
write(6,*)'The calculated value of b equals',b  
write(6,*)'The calculated rate factor (lambda/b) equals',ratef  
stop  
end  
C *****  
C *****
```



```
      write(7,*) time(i)
      write(8,*) strain(i)
      if (time(i).gt.100000.) dtime=10000.0
      if (time(i).gt.3000000.) dtime=100000.
      if (time(i).gt.10000000.) goto 20
10 continue
20 continue
      stop
      end
C *****
C *****
```

APPENDIX D: DESIGN EXAMPLES

APPENDIX D: DESIGN EXAMPLES

UNREINFORCED EMBANKMENT

This example illustrates the design of the unreinforced embankment shown in Figure D1.

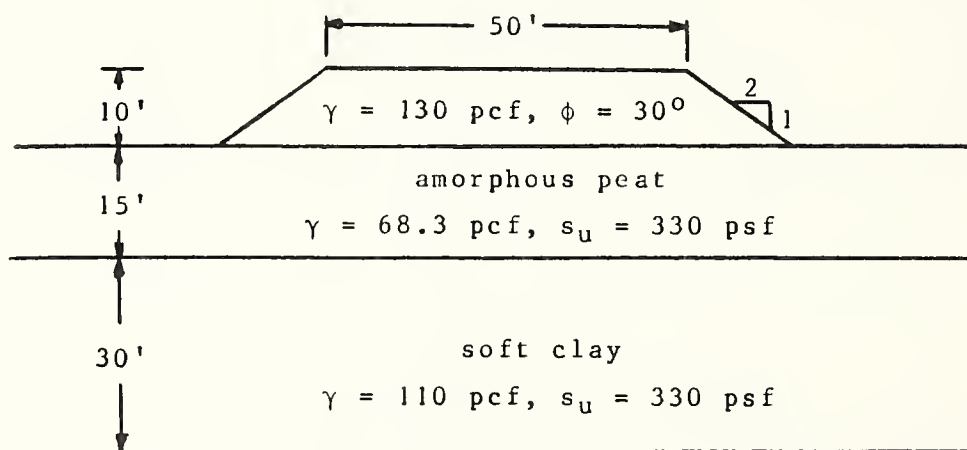


Figure D1 Embankment Configuration for Design Example.

Design Procedure

1. Overall Bearing Capacity:

$$q_{ult} = cN_c$$

$$N_c = 5.14 \text{ (pg. 112, Das 1984)}$$

$$q_{ult} = (330 \text{ psf})(5.14)$$

$$= 1696.2 \text{ psf}$$

$$q_{all} = \frac{1696.2}{1.3}$$

$$= 1304.8 \text{ psf}$$

Find allowable height:

$$H = \frac{q_{all}}{\gamma}$$

$$= \frac{1304.8 \text{ psf}}{130 \text{ pcf}} = 10.04 \text{ ft}$$

2. Lateral Squeeze:

$$P = \frac{1}{2} c B L^2$$

P = wt. of unit length of embankment

$$= \frac{1}{2} (90 + 50) (10 \text{ ft}) (130 \text{ pcf}) (1 \text{ ft})$$

$$= 91000 \text{ lb}$$

Find required shear strength to prevent lateral squeeze:

$$91000 = \frac{1}{7.5} c (1 \text{ ft}) (45 \text{ ft})^2$$

$$c_{req} = 337.0 \text{ psf}$$

Calculate factor of safety:

$$F.S. = \frac{c_{avail}}{c_{req}}$$

$$= \frac{330}{337}$$

$$= 0.98 < 1.3 \quad \text{NG}$$

At this point, there are two options. Either reduce the height of the first load, or decrease the embankment slope to widen the base. Try changing slope to 1:4 as shown in Figure D2.

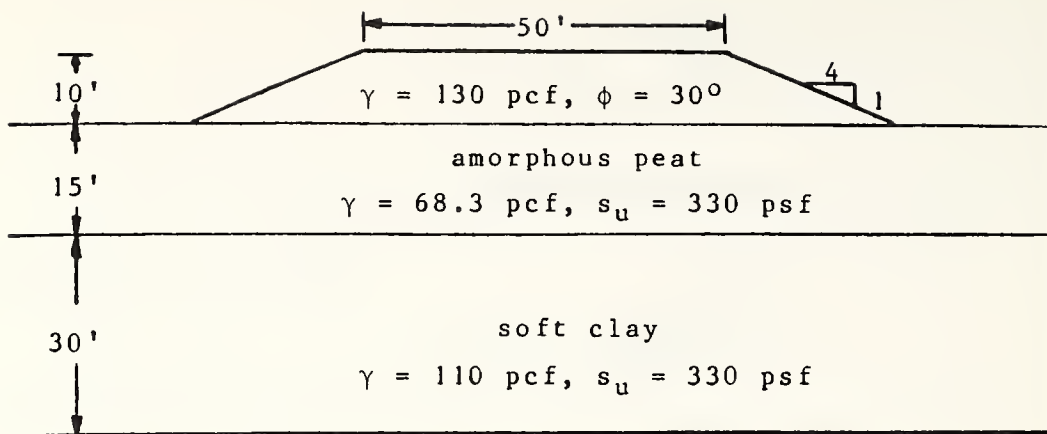


Figure D2 Revised Embankment Configuration for Design Example.

$$P = \frac{1}{2}(50+130)(10\text{ft})(130\text{pcf})(1\text{ft})$$

$$= 117,000 \text{ lb}$$

$$117,000 = \left(\frac{1}{7.5}\right)c(1\text{ft})(65\text{ft})^2$$

$$c_{\text{req}} = 207.7 \text{ psf}$$

$$\text{F.S.} = \frac{c_{\text{avail}}}{c_{\text{req}}}$$

$$= \frac{330}{207.7}$$

$$= 1.59 > 1.3 \quad \text{OK}$$

3. Embankment Spreading

The most crucial location for lateral spreading is at the crest of the embankment, as long as the slope is less than 1:1. At the crest, the lateral earth pressure is equal to the maximum value, yet the resistance to sliding is at a minimum.

Calculate lateral earth forces:

$$\begin{aligned}
 P_a &= \frac{1}{2} \gamma H^2 \tan^2 \left(45 - \frac{30}{2} \right) \\
 &= \frac{1}{2} (130) (10)^2 \tan^2 \left(45 - \frac{30}{2} \right) \\
 &= 2167 \text{ lb}
 \end{aligned}$$

Calculate resistive forces:

$$\begin{aligned}
 P_r &= cL \\
 &= 330(40) = 13200 \text{ lb}
 \end{aligned}$$

Calculate factor of safety:

$$\begin{aligned}
 F.S. &= \frac{P_r}{P_a} \\
 &= \frac{13200}{2167} \\
 &= 6.1 > 2.0 \quad \text{OK}
 \end{aligned}$$

4. Stability Analysis

Perform stability analysis using STABL4 or STABL5.

The input used is presented below, and the

resulting output is illustrated in Figure D3.

The calculated minimum factor of safety against rotational failure using the modified Bishop method is equal to $1.64 > 1.3$ OK.

```

profil
embankment stability
5 3
0.0 40.0 100.0 40.0 2
100.0 40.0 140.0 50.0 1
140.0 50.0 165.0 50.0 1
100.0 40.0 165.0 40.0 2
0.0 25.0 165.0 25.0 3
soil
3
130.0 130.0 0.0 30.0 0.0 0.0 1
68.3 68.3 330.0 0.0 0.0 0.0 1
110.0 110.0 330.0 0.0 0.0 0.0 1
water
1 62.4
2
0.0 40.0
165.0 40.0
circl2
5 30 60.0 95.0 110.0 155.0 0.0 2.5 0.0 0.0

```

5. Settlement Prediction

From the results of Creep Test OL-9-2, a plot of log strain rate versus time is constructed, as shown in Figure D4. The y-intercept and line slope are found as indicated on the Figure. These values are then used in GIBSON.F for calculation of the parameters required for the Gibson-Lo model.

GIBSON.F Input:

```
-4.95 0.000194 0.333557 2900.0 8.3
```

PLOT OF STABL output

10 most critical of surfaces generated
Minimum Factor of Safety = 1.635

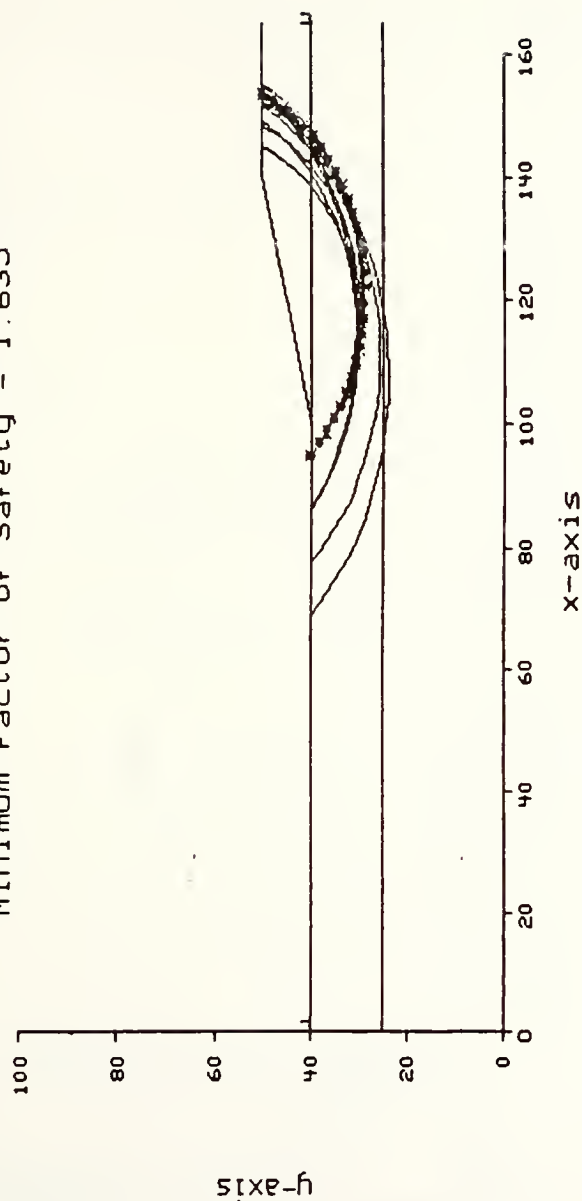


Figure D3 Plot of STABL Output for 10 Foot Embankment.

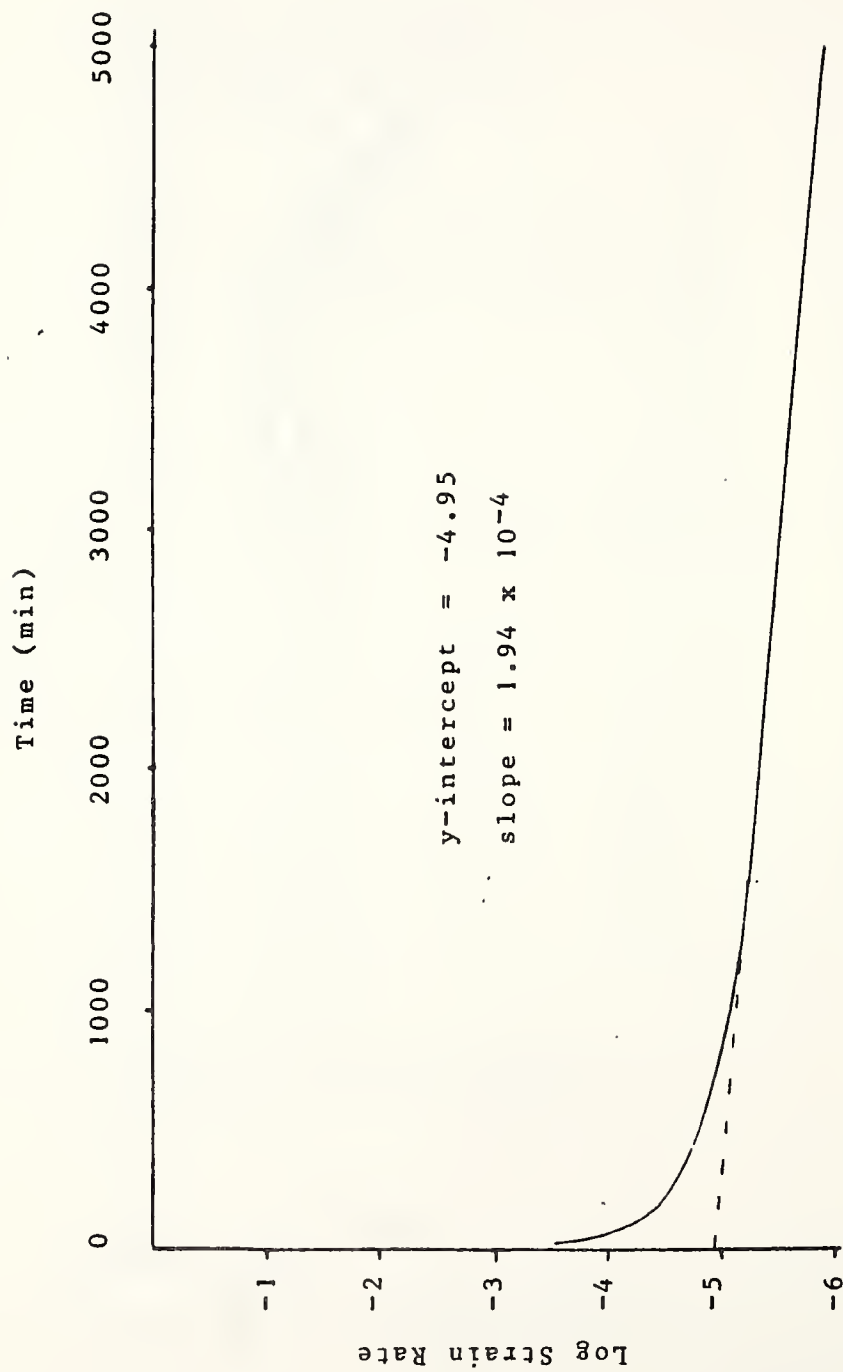


Figure D4 Plot of Logarithm Strain Rate Versus Time, Creep Test OL-9-2.

GIBSON.F OUTPUT

The calculated value of a equals 3.79906e-02
 The calculated value of b equals 3.02420e-03
 The calculated rate factor (λ/b) equals 4.47005e-04

These parameters must now be corrected for field conditions:

For this embankment, $\Delta\sigma=9.0$ psi.

From Figure 2.3,

$$\frac{b_{\text{field}}}{b_{\text{lab}}}=8.8$$

$$b_{\text{field}}=0.0266$$

Using $(\frac{\lambda}{b})_{\text{lab}}$, find the average

laboratory strain rate from Figure 2.4.

$$\text{Laboratory strain rate}=2.8 \times 10^{-5}$$

Edil & Mochtar (1984) recommend assuming a field strain rate two to three orders of magnitude smaller than the laboratory strain rate if field values are not known from previous experience.

$$\begin{aligned} \text{Try using field strain rate} &= \frac{2.8 \times 10^{-5}}{280} \\ &= 1 \times 10^{-7} \end{aligned}$$

From Figure 2.4,

$$(\frac{\lambda}{b})_{\text{field}}=2 \times 10^{-6}$$

Now, using SETTLE.F make settlement predictions.

SETTLE.F Input:

0.03799 0.0266 0.000002 9.0 1000.

From SETTLE.F Output, ultimate strain is equal to 0.58. A plot of strain versus time is shown in Figure D5.

6. Surcharge

Find maximum height of the second load. In order to accomplish this, a new round of field vane shear tests should be performed to find the strength gain beneath, and adjacent to the embankment.

For purposes of this example, assume

s_u beneath embankment = 500 psf

s_u adjacent to embankment = 400 psf

Stability analyses as illustrated in Steps 1 through 4 must now be performed to calculate the safe height of the surcharge.

Overall Bearing Capacity:

$$q_{ult} = cN_c, \text{ where } c = \text{average } s_u$$

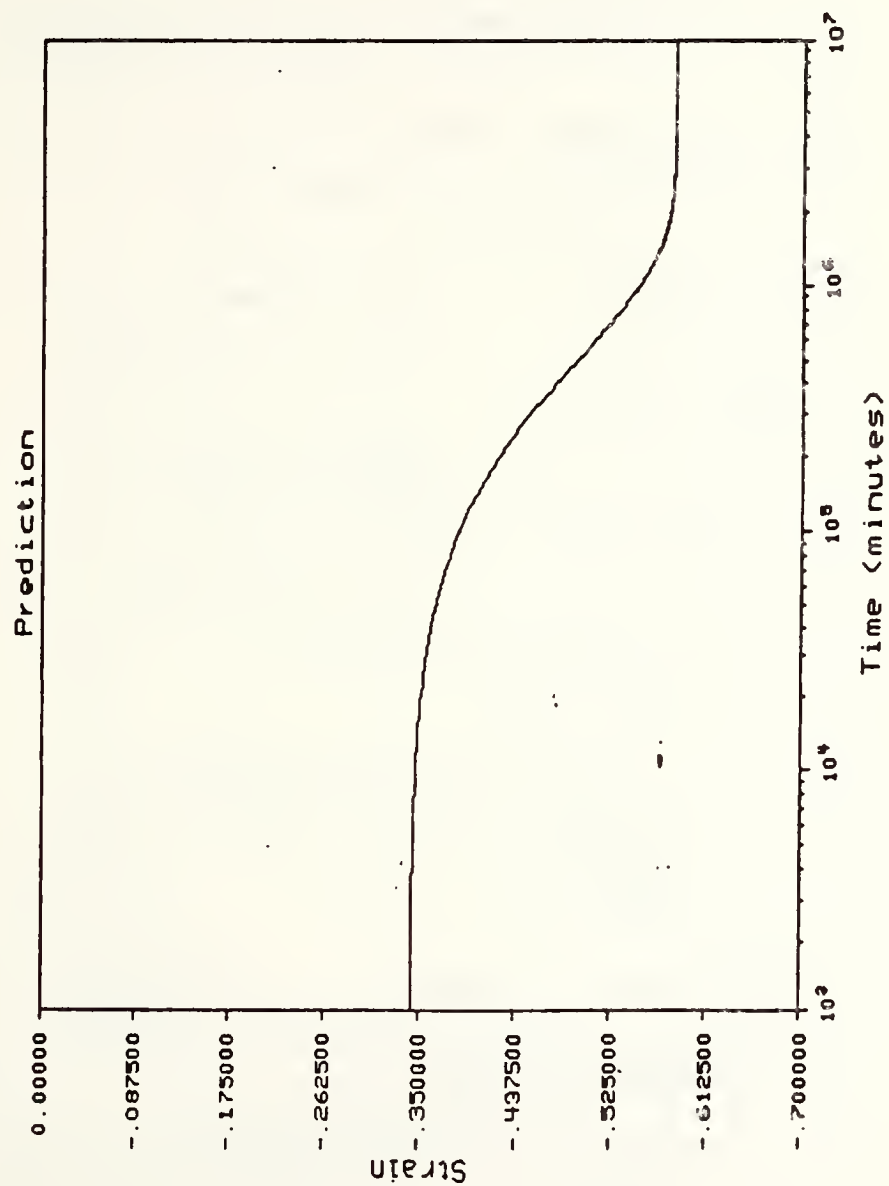


Figure D5 Settlement Prediction for 10 Foot Embankment.

$$c = \frac{400+500}{2} = 450 \text{ psf}$$

$$\begin{aligned} q_{ult} &= 450(5.14) \\ &= 2313.0 \text{ psf} \end{aligned}$$

$$\begin{aligned} q_{all} &= \frac{2313.0}{1.3} \\ &= 1779.2 \text{ psf} \end{aligned}$$

$$H = \frac{1779.2}{130} = 13.7 \text{ ft} \quad (\text{top width} = 20.4 \text{ ft})$$

Lateral Squeeze:

$$\begin{aligned} P &= \frac{1}{2}(130+20.4)(13.7 \text{ ft})(130 \text{ pcf}) \\ &= 133,931 \text{ lb} \end{aligned}$$

$$133,931 = \left(\frac{1}{7.5}\right)c(1 \text{ ft})(65 \text{ ft})^2$$

$$c_{req} = 237.7 \text{ psf}$$

$$\begin{aligned} FS &= \frac{c_{avail}}{c_{req}} \\ &= \frac{450}{237.7} = 1.89 > 1.3 \quad \text{OK} \end{aligned}$$

Embankment Spreading:

$$\begin{aligned} P_a &= \frac{1}{2}\gamma H^2 \tan^2\left(45 - \frac{\phi}{2}\right) \\ &= \frac{1}{2}(130)(13.7 \text{ ft})^2 \tan^2\left(45 - \frac{30}{2}\right) \\ &= 4067 \text{ lb} \end{aligned}$$

$$\begin{aligned} P_r &= cL \\ &= 450(54.8) \end{aligned}$$

=24660 lb

$$FS = \frac{24660}{4067} = 6.1 > 2.0 \quad OK$$

Stability Analysis:

The input used is shown below, and the resulting output is shown in Figure D6.

$$FS = 1.91 > 1.3 \quad OK$$

```

profil
embankment stability
8 3
0.0 40.0 100.0 40.0 4
100.0 40.0 154.8 53.7 1
154.8 53.7 165.0 53.7 1
100.0 40.0 127.4 40.0 4
127.4 40.0 165.0 40.0 2
0.0 25.0 126.4 25.0 3
126.4 25.0 127.4 40.0 2
126.4 25.0 165.0 25.0 3
soil
4
130.0 130.0 0.0 30.0 0.0 0.0 1
68.3 68.3 500.0 0.0 0.0 0.0 1
110.0 110.0 330.0 0.0 0.0 0.0 1
68.3 68.3 400.0 0.0 0.0 0.0 1
water
1 62.4
2
0.0 40.0
165.0 40.0
circl2
5 30 60.0 95.0 110.0 155.0 0.0 2.5 0.0 0.0

```

Prediction Analysis:

According to Gruen & Lovell (1983), the parameters of the Gibson-Lo model are valid for stress levels less than twice that used during testing for

PLOT OF STABL output

10 most critical of surfaces generated
Minimum Factor of Safety = 1.913

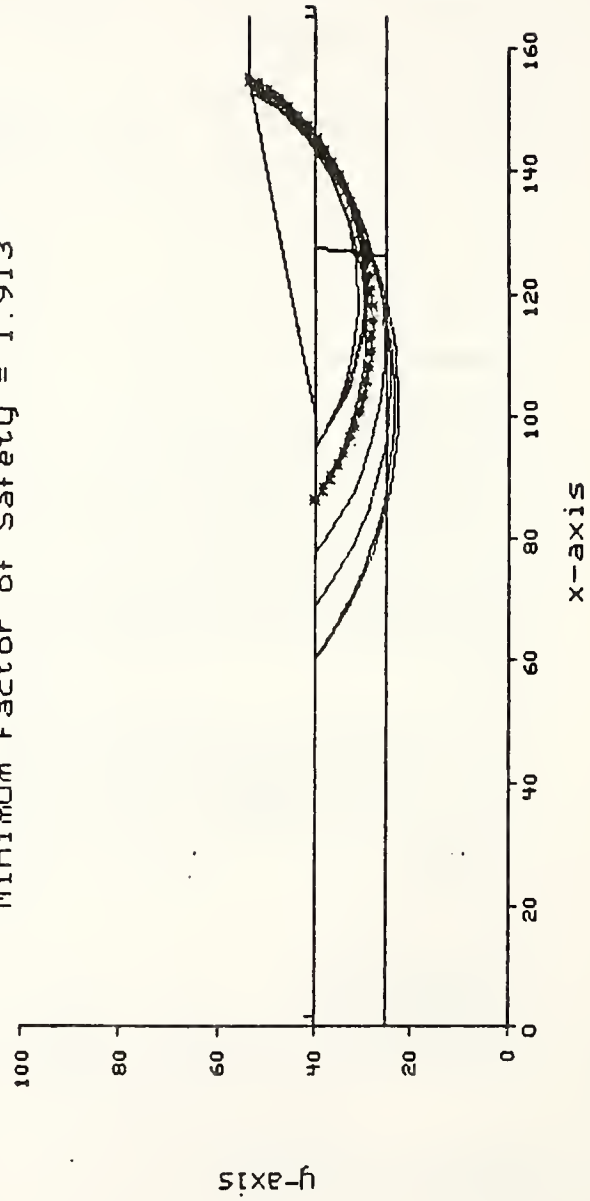


Figure D6 Plot of STABL Output for Surcharged Embankment.

initial determination of these parameters.

$\Delta\sigma = 12.37 \text{ psi} < 2 \times 8.3 \text{ psi}$ OK

A settlement prediction is now performed using SETTLE.F.

SETTLE.F Input:

0.03799 0.0266 0.000002 12.37 1000.

The resulting settlement prediction is illustrated in Figure D7. From this Figure, it is observed that the strain occurring during the service life of the 10 foot high embankment will occur in approximately 200,000 minutes, or 4.6 months. Therefore, after the surcharge is applied for approximately 5 months, it can be removed, and settlements will be minimal.

GEOTEXTILE REINFORCED EMBANKMENT

This example will illustrate the design of the embankment in the first example when geotextiles are to be used at the base.

Design Procedure

1. Overall Bearing Capacity:

As a result of the geotextile, the pressure resulting from the embankment can be calculated as the total load, P , over the length of the embankment, $2L$. Check

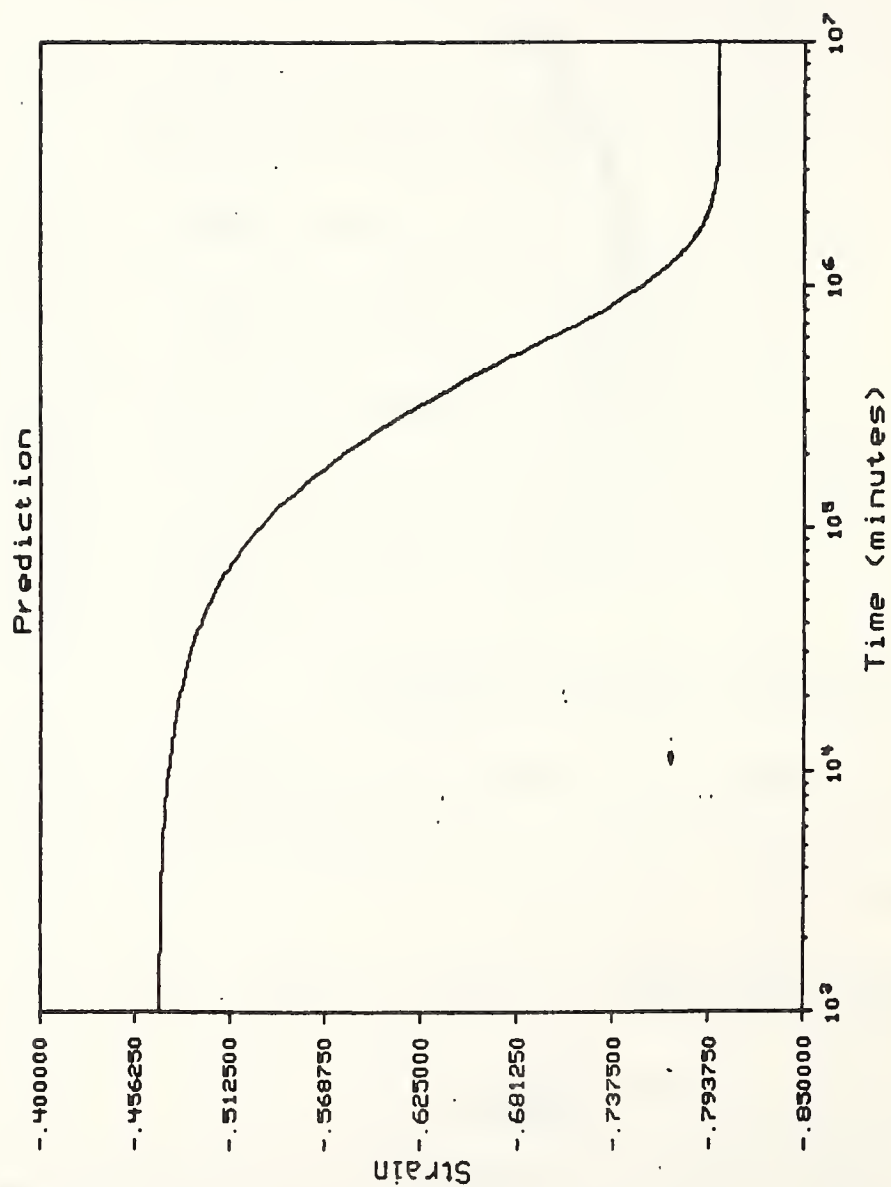


Figure D7 Settlement Prediction for Surcharged Embankment.

to see if the entire load, including the preload, can be applied in one stage.

$$q_{ult} = 1696.2 \text{ psf}$$

$$q_{app} = \frac{P}{(L)(1)}$$

$$P = 133,931 \text{ lb}$$

$$q_{app} = \frac{133,931}{130}$$

$$= 1030 \text{ psf}$$

$$FS = \frac{1696.2}{1030.2}$$

$$= 1.65 > 1.3 \quad \text{OK}$$

2. Lateral Squeeze:

$$c_{req} = 237.7 \text{ psf}$$

$$c_{avail} = 330.0 \text{ psf}$$

$$FS = \frac{330.0}{237.7}$$

$$= 1.39 > 1.30 \quad \text{OK}$$

3. Embankment Spreading:

$$P_a = 4067 \text{ lb}$$

$$P_r = \frac{1}{2} \gamma L H \tan \phi_{sf}$$

$$= \frac{1}{2} (130) (54.8) (13.7) \tan \phi_{sf}$$

$$\phi_{sf} = \tan^{-1} \left(\frac{4P_a}{\gamma} L H \right)$$

$$= \tan^{-1} \left[\frac{(4)(4067)}{(130)(54.8)(13.7)} \right]$$

$$= 9.46^\circ < \frac{2}{3} \phi$$

$$\text{Specify } \phi_{sf} = 20^\circ$$

$$P_r = \frac{1}{2} (130) (54.8) (13.7) \tan 20^\circ$$

$$= 17762 \text{ lb}$$

$$FS = \frac{17762}{4067}$$

$$= 4.4 > 2.0 \quad \text{OK}$$

4. Stability Analysis:

Perform the stability analysis using STABL6. The input used is presented below, as well as a list of points defining the most critical failure surface. The calculated minimum factor of safety against rotational failure without a geotextile is 1.31. Therefore, the geotextile will not be necessary to resist rotational failure.

```

PROFIL
REINFORCED EMBANKMENT STABILITY
5 3
0.0 40.0 100.0 40.0 2
100.0 40.0 154.8 53.7 1
154.8 53.7 176.0 53.7 1
100.0 40.0 176.0 40.0 2
0.0 25.0 176.0 25.0 3
SDIL
3
130.0 130.0 0.0 30.0 0.0 0.0 1
68.3 68.3 330.0 0.0 0.0 0.0 1
110.0 110.0 330.0 0.0 0.0 0.0 1
WATER
1 62.4
2
0.0 40.0
176.0 40.0
REINF
1
3
100.0 40.0 0.0 0.0
156.0 40.0 00.0 0.0
176.0 40.0 00.0 0.0
CIRCL2
5 30 60.0 95.0 110.0 165.0 0.0 2.5 0.0 0.0
EXECUT

```

5. Find Required Fabric Strength:

Since the geotextile is not required to resist rotational failure, the required fabric strength is controlled by the forces developed in the fabric as a result of embankment spreading.

$$T_f = 1.5 P_a$$

Following Are Displayed The Ten Most Critical Of The Trial Failure Surfaces Examined. They Are Ordered - Most Critical First.

* * Safety Factors Are Calculated By The Modified Bishop Method * *

Failure Surface Specified By 35 Coordinate Points

Point No.	X-Surf (ft)	Y-Surf (ft)
1	95.00	40.00
2	96.78	38.24
3	98.66	36.59
4	100.63	35.06
5	102.69	33.64
6	104.83	32.35
7	107.04	31.19
8	109.32	30.16
9	111.66	29.26
10	114.04	28.51
11	116.46	27.90
12	118.92	27.43
13	121.40	27.10
14	123.89	26.93
15	126.39	26.90
16	128.89	27.02
17	131.38	27.29
18	133.84	27.70
19	136.28	28.26
20	138.68	28.96
21	141.03	29.80
22	143.33	30.78
23	145.57	31.90
24	147.74	33.14
25	149.83	34.51
26	151.84	36.00
27	153.75	37.61
28	155.57	39.33
29	157.28	41.15
30	158.88	43.07
31	160.37	45.08
32	161.73	47.17
33	162.97	49.34
34	164.08	51.59
35	164.97	53.70

Circle Center At X = 125.6 ; Y = 69.2 and Radius, 42.3

*** 1.310 ***

$$=1.5(4067)$$

$$=6100 \text{ lb}$$

6. Find Required Geotextile Tensile Modulus:

$$E_f = (6100)(10)$$

$$=61,000 \text{ psf}$$

7. Settlement Prediction:

The use of a geotextile will not affect the total settlements experienced beneath the embankment.

Therefore, the prediction made in the previous example for the surcharged height of embankment is still valid.

APPENDIX E: NEGATIVE NUMBERS FOR CONTACT PRINTS

APPENDIX E: NEGATIVE NUMBERS FOR CONTACT PRINTS

Figure	Negative Number	Location of Negative
3.1	1 *	Stewart Center, Room 65
3.2	25 *	Stewart Center, Room 65
3.6	9 *	Stewart Center, Room 65
3.7	14 *	Stewart Center, Room 65
3.8	26	Grissom Hall, Room 140

* Information required for retrieval:

3/30/87 Civil Engineering-Tim Crawl-Equipment 35

COVER DESIGN BY ALDO GIORGINI